

UNIVERSIDADE FEDERAL DO PARANÁ

ANTONIO IRINEUDO MAGALHÃES JÚNIOR

RECOVERY OF ITACONIC ACID FROM AQUEOUS SOLUTIONS

CURITIBA

2015

ANTONIO IRINEUDO MAGALHÃES JÚNIOR

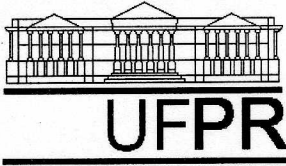
RECOVERY OF ITACONIC ACID FROM AQUEOUS SOLUTIONS

Dissertação apresentada como requisito parcial à obtenção do grau de Mestre em Engenharia de Bioprocessos e Biotecnologia, no Programa de Pós-Graduação em Engenharia de Bioprocessos e Biotecnologia, Setor de Tecnologia, da Universidade Federal do Paraná.

Orientador: Prof. Dr. Júlio Cesar de Carvalho

CURITIBA

2015



RELATÓRIO DE DEFESA DE DISSERTAÇÃO DE MESTRADO

Aos vinte e sete dias do mês de Março de 2015, na Sala 1 do prédio Cenbapar, no Setor de Tecnologia do Centro Politécnico da Universidade Federal do Paraná, Jardim das Américas, foi instalada pelo Prof. Dr. Júlio César de Carvalho, Coordenador do Programa de Pós-Graduação em Engenharia de Bioprocessos e Biotecnologia, a banca examinadora para a Nonagésima Nona Defesa de Dissertação de Mestrado, área de concentração: Agroindústria e Biocombustíveis. Estiveram presentes no Ato, além do Coordenador do Curso de Pós-Graduação, professores, alunos e visitantes.

A Banca Examinadora, atendendo determinação do Colegiado do Curso de Pós-Graduação em Engenharia de Bioprocessos e Biotecnologia ficou constituída pelos membros: Profa. Dra. Luciana Porto de Souza Vandenberghe (UFPR), Prof^a Dra. Cristine Rodrigues (UFPR), Profa. Dra. Susan Grace Karp (UP), e Prof^o Dr. Júlio Cesar. de Carvalho (UFPR – orientador da dissertação).

Às 14h00, a banca iniciou os trabalhos, convidando o candidato **Antônio Irineudo Magalhães Júnior** a fazer a apresentação da dissertação intitulada: **“RECOVERY OF ITACONIC ACID FROM AQUEOUS SOLUTIONS”**. Encerrada a apresentação, iniciou-se a fase de arguição pelos membros participantes.

Tendo em vista a dissertação e a arguição, a banca composta pelos membros Prof^a Dra. Luciana Porto de Souza Vandenberghe, Prof^a Dra. Cristine Rodrigues, Profa. Dra. Susan Grace Karp e Prof^o Dr. Júlio Cesar de Carvalho, declarou o candidato APROVADO (de acordo com a determinação dos Artigos 59 a 68 da Resolução 65/09 de 30.10.09).

Curitiba, 27 de Março de 2015.



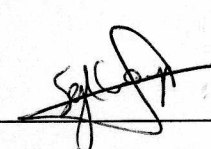
Prof. Dr. Júlio Cesar de Carvalho



Profa. Dra. Luciana P. S. Vandenberghe



Profa. Dra. Cristine Rodrigues



Profa. Dra. Susan Grace Karp

Aos meus pilares: Antonio, Elza, Ana e Arthur.

AGRADECIMENTOS

Ao Programa de Pós-Graduação e ao Departamento de Engenharia de Bioprocessos e Biotecnologia, à Universidade Federal do Paraná, seu corpo docente, direção e administração que abriram suas portas para tornar-me engenheiro e agora, mais uma vez, para a obtenção do grau de Mestre em Engenharia de Bioprocessos e Biotecnologia.

À Coordenação de Aperfeiçoamento de Pessoal de Nível Superior (CAPES) e ao Conselho Nacional de Desenvolvimento Científico e Tecnológico (CNPq) pelo suporte financeiro concedido para a realização deste trabalho.

Ao Prof. Dr. Júlio César de Carvalho pela orientação, apoio, confiança e oportunidade na elaboração deste trabalho.

Aos meus companheiros científicos, Jesus David Coral Medina, André Luiz Gollo, Gilberto Vinícius de Melo Pereira, Marcela Candido Câmara, Liliana Isabel Chitolina Zoz, por tornar o ambiente de laboratório criativo e amigável.

Aos meus pais, Elza Satiko Oyagawa Magalhães e Antonio Irineudo Magalhães, por sempre acreditarem em mim.

Aos meus irmãos, sobrinhos, sogros e cunhados, pelo apoio incondicional.

Ao meu filho, Arthur José Collaço Magalhães, por sua criatividade e empolgação.

À minha amada, Ana Carolina Lazzaron Collaço, pela paciência, dedicação, suporte, correções e revisões.

“Stay hungry. Stay foolish”
(Steve Jobs apud Whole Earth Catalog)

RESUMO

Ácido itacônico (AI) é um produto químico promissor que tem uma ampla gama de aplicações e pode ser obtido em grande escala por processos fermentativos. A separação de AI a partir do caldo fermentativo tem um impacto considerável no custo total da produção. Por conseguinte, a procura de processos para a recuperação de ácidos orgânicos com alta eficiência e baixo custo é um dos passos chave para a substituição de produtos de base petroquímica. Apesar dos avanços biotecnológicos em frente aos processos fermentativos, o principal obstáculo ainda é a separação e purificação. Uma revisão sobre os principais métodos de separação foi realizada nesse trabalho e fomentou as diretrizes dessa investigação. Um dos métodos mais comuns para a separação de ácidos orgânicos envolve a precipitação e ressolubilização (regeneração). Os estudos sobre a precipitação de AI são dificilmente encontrados na literatura, embora estejam bem desenvolvidos. Neste estudo, os dados da solubilidade de itaconato de cálcio foram determinados de modo a avaliar o potencial de precipitação de AI. O processo foi muito dependente da temperatura, com recuperação de 88 a 97% na faixa de 20 a 80°C. A separação de AI a partir de soluções aquosas usando resinas comerciais de troca iônica fortemente básicas foi outra investigação realizada. A adsorção foi investigada para determinar os efeitos da concentração inicial de AI, pH e temperatura. As isotermas clássicas de Freundlich e Langmuir e a cinética de pseudo-segunda ordem foram utilizadas para calcular os parâmetros de adsorção. Um modelo matemático simplificado foi desenvolvido e validado com dados experimentais de uma coluna de leito fixo. Durante os experimentos, um método analítico foi desenvolvido para a determinação da concentração de AI em solução aquosa.

Palavras-chave: Recuperação de Ácidos Orgânicos, Ácido Itacônico, Análise, Precipitação, Adsorção.

ABSTRACT

Itaconic acid (IA) is a promising chemical product, which has a wide range of applications and can be obtained in large scale by fermentative processes. The separation of IA from fermented broth has a considerable impact in the total cost of production. In that way, the search for high efficiency and low cost processes of organic acids recovery is one of the key steps to the replacement of petrochemical-based products. Despite the important biotechnological advances in fermentative processes, the biggest remaining obstacles remain being the separation and purification. In this work, a review of the main separation methods has been done showing that the most common methods of organic acids separation involves precipitation and regeneration. Studies about IA precipitation are rare in the literature. In this study, the data about calcium itaconate solubility were determined as a means to evaluate IA precipitation potential. The process is dramatically dependent of temperature, with recovering yields ranging from 88 to 97% at temperatures of 20 to 80°C. Another investigation made was the IA separation from aqueous solutions using strongly basic commercial ion-exchange resins. This adsorption method was investigated in order to determine the effects of IA initial concentration, pH and temperature. The classical isotherms of Freundlich and Langmuir and a pseudo-second order kinetics were used to calculate the adsorption parameters. A simplified mathematical model was developed and evaluated with experimental data obtained from a fixed bed column. During the experiments, an analytical method was developed to determine the concentration of IA in aqueous solution.

Key words: Organic Acids Recovery, Itaconic Acid, Analysis, Precipitation, Adsorption.

FIGURE INDEX

FIGURE 2.1. Chemical structure of IA.....	18
FIGURE 2.2. IA solubility in water at different temperatures	19
FIGURE 2.3. Schematic diagram of IA recovery process from fermentative broth....	20
FIGURE 3.1. Schematic diagram for the preparation of the sodium itaconate salt....	29
FIGURE 3.2. Schematic diagram for the spectrophotometric analysis for transition metal selection with potential complexation with itaconate.....	30
FIGURE 3.3. Effect of pH on the itaconic acid deprotonation.....	32
FIGURE 3.4. Effect of itaconate in the scanning spectrophotometric of different metal transition.....	34
FIGURE 3.5. Spectrophotometry of solutions with different concentrations of sodium itaconate-cobalt chloride	35
FIGURE 3.6. Job's method applied to different proportions of sodium itaconate and cobalt chloride	36
FIGURE 3.7. Spectrophotometry of solutions with different concentrations of sodium itaconate:nickel sulfate	36
FIGURE 3.8. Job's method applied to different proportions of sodium itaconate and nickel sulfate.....	37
FIGURE 3.9. Spectrophotometry of solutions with different concentrations of sodium itaconate/ copper chloride	38
FIGURE 3.10. Job's method applied to different proportions of sodium itaconate and copper chloride.....	38
FIGURE 3.11. Effect of different pH in the absorbance of sodium itaconate-chloride copper	39
FIGURE 3.12. Effect of different pH copper-itaconate complex and copper chloride	39
FIGURE 3.13. Effect of concentration of mix on the precipitation.....	40
FIGURE 3.14. Concentration curve of itaconate.	41
FIGURE 4.1. Effect of temperature on the solubility of calcium hydroxide in water...	44
FIGURE 4.2. Schematic diagram for the preparation of the calcium itaconate salt ...	45
FIGURE 4.3. Schematic diagram for the determination of the solubility of calcium itaconate.....	46
FIGURE 4.4. UV spectra of itaconate at several concentrations	48

FIGURE 4.5. Absorbance of itaconate as a function of concentration.....	48
FIGURE 4.6. Solubility of calcium itaconate at different temperatures	50
FIGURE 4.7. Yield of itaconate recovery versus sulfuric acid concentration	51
FIGURE 5.1. Determination of the batch's adsorption parameters.....	56
FIGURE 5.2. Experimental fixed-bed continuous adsorption	59
FIGURE 5.3. Scheme of the main stages and directions in the mass transfer of the fixed bed adsorption column.....	60
FIGURE 5.4. Mass transfer in accordance with the movement through the adsorption bed	61
FIGURE 5.5. Effect of initial pH on the adsorption of IA onto ion-exchange resins ...	65
FIGURE 5.6. Effect of temperature on the adsorption of IA onto ion-exchange resins	66
FIGURE 5.7. Langmuir isotherm for the adsorption of IA onto ion-exchange resins .	68
FIGURE 5.8. Freundlich isotherm for the adsorption of IA onto ion-exchange resins	69
FIGURE 5.9. Pseudo-Second Order equation for the adsorption kinetics of IA onto ion-exchange resins	71
FIGURE 5.10. IA concentration in the fixed bed column outlet (C_f).....	72
FIGURE 5.11. Relation between adsorption and IA concentration in the fixed bed column outlet.....	73
FIGURE 5.12. IA elution from ion-exchange resins in fixed bed column.	74
FIGURE 5.13. Mathematical model of the fixed bed column.....	75
FIGURE 6.1. Process flow design of IA recovery process from fermentative broth with adsorption fixed bed column.....	78

TABLE INDEX

TABLE 2.1. Recovery yields of IA (%) in specific downstream steps described in literature	21
TABLE 2.2. Main process of IA recovery.....	26
TABLE 3.1. Concentration of transition metals and itaconate used to prepare Jobs Graphic.....	31
TABLE 3.2. Tests of the effect of copper concentration on the precipitation with itaconate.....	32
TABLE 3.3. Determination of the concentration curve of itaconate	41
TABLE 4.1. Solubility of calcium itaconate at different temperatures	50
TABLE 4.2. Test results of the dissolution of itaconate with sulfuric acid at different concentrations	51
TABLE 5.1. Typical physical and chemical characteristics of the resins	56
TABLE 5.2. Effect of initial pH on the adsorption of IA onto ion-exchange resins	64
TABLE 5.3. Effect of temperature on the adsorption of IA onto ion-exchange resins	66
TABLE 5.4. Effect of initial concentration of acid on the adsorption of IA onto ion-exchange resins	67
TABLE 5.5. Langmuir isotherm parameters for the adsorption of IA onto ion-exchange resins	68
TABLE 5.6. Freundlich isotherm parameters for the adsorption of IA by ion-exchange resins.....	69
TABLE 5.7. Effect of contact time of IA on the adsorption.....	70
TABLE 5.8. Pseudo-Second Order Equation parameters for the adsorption kinetics of IA onto ion-exchange resins	71
TABLE 5.9. Calculated values of the experimental fixed bed column model parameters	75

SUMMARY

1. GENERAL INTRODUCTION	15
2. RECOVERY OF BIOTECHNOLOGICALLY PRODUCED ITACONIC ACID: A REVIEW	17
2.1. ABSTRACT	17
2.2. INTRODUCTION.....	17
2.3. PHYSICAL AND CHEMICAL PROPERTIES	18
2.4. CLASSICAL RECOVERY METHODS	19
2.4.1. Crystallization.....	19
2.4.2. Precipitation	21
2.4.3. Liquid-Liquid Extraction.....	22
2.4.4. Electrodialysis	23
2.4.5. Diafiltration	24
2.4.6. Pertraction	25
2.4.7. Adsorption.....	25
2.5. CONCLUSIONS.....	25
3. SPECTROPHOTOMETRIC METHOD FOR DETERMINING ITACONIC ACID BY COMPLEXES FROM TRANSITION METALS.....	27
3.1. ABSTRACT	27
3.2. INTRODUCTION.....	27
3.3. MATERIALS AND METHODS	29
3.3.1. Selection of Transition Metals	29
3.3.2. Job's Method	30
3.3.3. pH Effect	31
3.4. RESULTS AND DISCUSSION.....	33
3.4.1. Transition Metal Selection with Potential Complexation with Itaconate.....	33
3.4.2. Determining of the Optimum Component Proportion for Each Complex...	34
3.4.3. Effect of pH on the Absorbance of the Complex	38
3.4.4. Determination of the Concentration Curve	40
3.5. CONCLUSIONS.....	41
4. PRECIPITATION OF CALCIUM ITACONATE AND DETERMINATION OF ITS SOLUBILITY AT DIFFERENT TEMPERATURES.....	43

4.1. ABSTRACT	43
4.2. INTRODUCTION.....	43
4.3. MATERIAL AND METHODS.....	45
4.3.1. Preparation and Recovery of Calcium Itaconate.....	45
4.3.2. Determination of Itaconate Concentration by Spectrophotometry.....	46
4.3.3. Determination of the Solubility of Calcium Itaconate.....	46
4.3.4. Regeneration of IA from Its Calcium Salt	47
4.4. RESULTS AND DISCUSSION.....	47
4.4.1. Determination of Concentration Curves for Itaconate by Spectrophotometric Method.....	47
4.4.2. Solubility of Calcium Itaconate	49
4.4.3. IA Regeneration	50
4.5. CONCLUSIONS.....	52
5. SEPARATION OF ITACONIC ACID FROM AQUEOUS SOLUTION ONTO ION- EXCHANGE RESINS.....	53
5.1. ABSTRACT	53
5.2. INTRODUCTION.....	54
5.3. MATERIAL AND METHODS.....	55
5.3.1. Determination of the Batch's Adsorption Parameters	55
5.3.2. Determination of Adsorption Isotherms.....	56
5.3.3. Determination of the Fixed-Bed Continuous Adsorption Parameters.....	59
5.3.4. Mathematical modeling of the fixed bed adsorption column	60
5.4. RESULTS AND DISCUSSION.....	63
5.4.1. Effect of pH in the Adsorption	63
5.4.2. Effect of Temperature in the Adsorption	65
5.4.3. Effect of Initial Acid Concentration in the Adsorption	66
5.4.4. Langmuir Isotherm	67
5.4.5. Freundlich Isotherm	68
5.4.6. Effect of Contact Time on the Adsorption	69
5.4.7. Pseudo-Second Order Equation	70
5.4.8. Fixed-Bed Continuous Adsorption Parameters.....	71
5.4.9. Determination of the Mathematical Model of the Fixed Bed Adsorption Column	74
5.5. CONCLUSIONS.....	75

6. GENERAL CONCLUSION AND FUTURE OUTLOOK.....	77
7. REFERENCES.....	79
APPENDIX.....	84

1. GENERAL INTRODUCTION

For many years, organic acids have played a key role as products in the chemical and food industry. The current interest in a renewable economy and the development of biotechnology has stimulated a significant change in the petrochemical-based products processes. The organic acids which currently are produced on an industrial scale by fermentation are citric, lactic, D-gluconic, itaconic, 2-keto-L-gulonic and succinic acids. (SOCCOL et al., 2006; MILLER et al., 2011; ROGERS et al., 2006; KLEMENT and BÜCHS, 2013; CUI et al., 2012; MCKINLAY et al., 2007).

The raw material and other upstream costs are the main responsible for the final price in the production of organic acids. However, downstream processes, such as recovery and purification, result in 30 to 40% of the final product cost (STRAATHOF, 2011). Thus, a competitive bioprocess is highly dependent on the development of efficient recovery and low cost processes (LÓPEZ-GARZÓN and STRAATHOF, 2014).

Itaconic acid (IA) is one prominent example that illustrates the obstacles and opportunities of a competitive biotechnological process. Although its biotechnological production is already industrially established, there are several studies being done regarding improvements in its fermentative and recovery steps (HUANG et al., 2014; KLEMENT et al., 2012; KUENZ et al., 2012; WANG et al., 2011; WASEWAR et al., 2011; CARSTENSEN et al., 2013; LI et al., 2013). The price of IA ranges between US\$1.6 to 2.0kg⁻¹ depending on the supplier, quality and purity. In 2011, the global market of itaconic acid was estimated at 41,400 tons (OKABE et al., 2009).

IA is produced by the fermentation of pre-treated sugarcane molasses with *Aspergillus terreus*, but it also can be produced through pyrolysis and controlled distillation of citric acid. The biotechnological path is mainly chosen due to the small price difference between IA and citric acid (WILLKE and VORLOP, 2001), which diminishes the economical efficiency of the chemical process (KLEMENT and BÜCHS, 2013). The fermented broth is filtered in order to remove mycelia and suspended solids. Thus, IA can be easily recovered using steps of broths evaporation and crystallization, with yield of approximately 75%. However, these methods do not remove fermentation subproducts, which diminish the product final

purity. The purification can be carried out by discoloration with activated carbon, reaching 99% purity (OKABE et al., 2009).

This study aimed to find an IA recovery method from the fermented broth. In order to reach that, Chapter 2 is a review that presents an analysis of the studies about bioprocess made IA recovery. This research led to the premises, which provided the underlying bases for Chapters 4 and 5. Chapter 3 brings us the development of a colorimetric method to quantify IA in aqueous solutions through spectrophotometric reading in visible wavelength.

The IA precipitation was investigated in Chapter 4. Despite the fact that there are well-known organic acid precipitation methods, the data about those methods is difficult to access. Thus, that Chapter aimed at determining such data through determination of sodium itaconate solubility. Adsorption is a promising recovery method, whose use was largely investigated to separate and purify other carboxylic acids, such as succinic, acetic and lactic. However, it was seldom studied for IA. Chapter 5 aimed to evaluate the IA separation using two ion exchange resins.

2. RECOVERY OF BIOTECHNOLOGICALLY PRODUCED ITACONIC ACID: A REVIEW

2.1. ABSTRACT

Itaconic acid (IA) is a promising chemical that has a wide range of applications and can be obtained in a large scale by fermentation processes. Separation of IA from fermentation broth has a considerable impact in the total cost of production. This review describes the current state of art of recovery and purification methods for IA production by bioprocesses. Previous studies on the separation of IA include crystallization, precipitation, extraction, electrodialysis, diafiltration, pertraction and adsorption. Although some of these studies show advances in separation and recovery methods, there is room for development in specific operations and in process integration.

2.2. INTRODUCTION

Itaconic acid (IA) is an organic acid with two carboxyl groups, and a carbon-carbon double bond. This diversity of functional groups allows a high diversity of reactions, such as complexation with metal ions, esterification with alcohols, production of anhydrides and polymerization (KUENZ et al., 2012). Therefore, IA may be used as a replacement for petroleum-based compounds such as acrylic or methacrylic acid (WILLKE and VORLOP, 2001). IA and its derivatives may be used in a large variety of industrial applications, such as co-monomers in resins and in the manufacture of synthetic fibers, in coatings, adhesives, thickeners and binders (WILLKE and VORLOP, 2001; OKABE, 2009).

Biotechnological advances have made possible the production of IA through fermentation using *Aspergillus terreus*, creating a renewable and environmentally friendly substitute to petrochemical-based products (WILLKE and VORLOP, 2001). However, some methods of separation and recovery of organic acids from the

fermentation broth are inefficient or highly costly, causing an increase in the final cost of production. The development of economically viable downstream process is paramount to allow bio-based production of an organic acid (LÓPES-GARZÓN and STRAATHOF, 2014). Crystallization methods are the most usual unit processes for recovery of IA. However, other recovery methods, such as extraction, electrodialysis, precipitation and adsorption are investigated. This survey aims to analyze the studies for recovery of IA from fermented broth.

2.3. PHYSICAL AND CHEMICAL PROPERTIES

Itaconic acid (IA) is a white, crystalline, monounsaturated organic diacid with formula $C_5H_6O_4$ (FIGURE 2.1) and a molar mass of $130.1g.mol^{-1}$, with solubility in water of $83.103g.l^{-1}$ at $20\text{ }^{\circ}C$. Its melting and boiling points are, respectively, 167 and $268^{\circ}C$. IA has three different states of protonation with dissociation constants in aqueous solutions of pK_{a1} ($3.66-3.89$) and pK_{a2} ($5.21-5.55$) (ROBERTIS et al., 1990; WILLKE and VORLOP 2001). The solubility of IA is extremely variable and highly dependent on temperature. FIGURE 2.2 shows experimental data on the solubility of the IA in water at various temperatures (APELBLAT and MANZUROLA, 1997; KRIVANKOVA et al., 1992). This feature enables methods of concentration and crystallization at high and low temperatures, respectively.

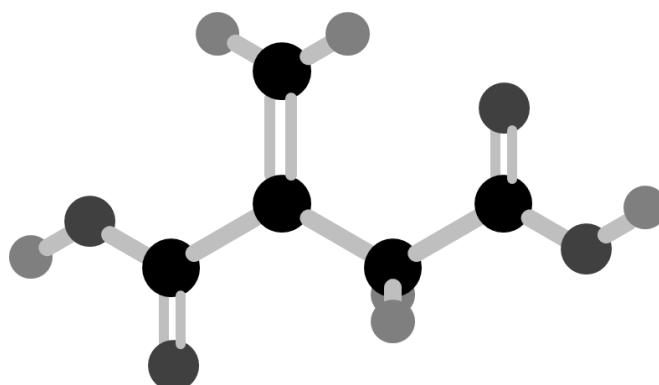


FIGURE 2.1. Chemical structure of IA.

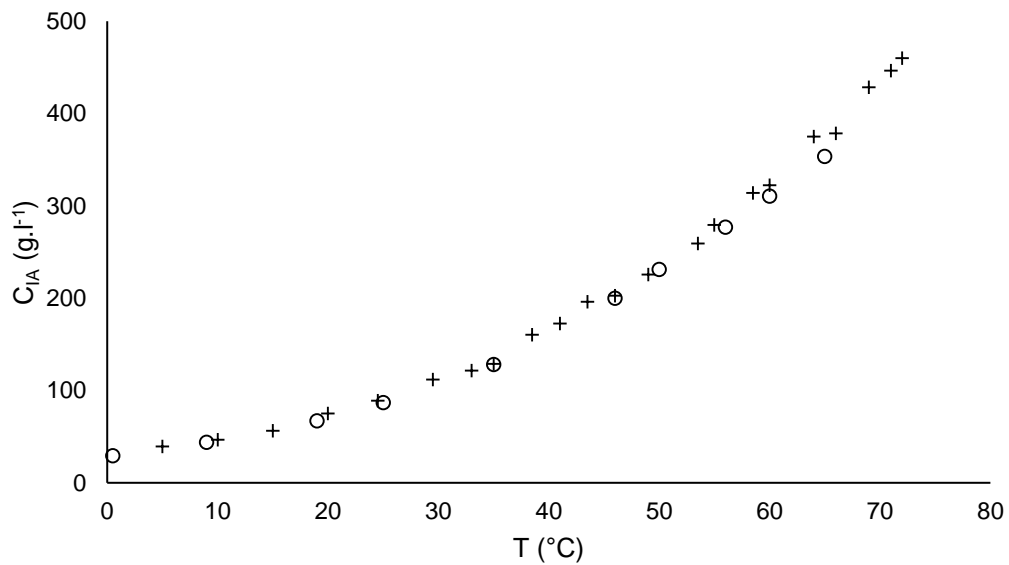


FIGURE 2.2. IA solubility in water at different temperatures (+) APELBLAT and MANZUROLA (1997); (o) KRIVANKOVA et al. (1992).

2.4. CLASSICAL RECOVERY METHODS

2.4.1. Crystallization

The classical method of IA recovery produced by fermentation processes is crystallization. IA can be easily recovered through this method by cooling or evaporation-crystallization, but both treatments do not separate other products of fermentation causing a decrease in the products final quality (KLEMENT and BÜCHS, 2013).

The industrial IA crystallization process was described by LOCKWOOD (1975), WILLKE and VORLOP (2001) and OKABE (2009) and is shown in FIGURE 2.3. Initially, the fermented broth is filtered to remove mycelia and other suspended solids. Then the filtrate is concentrated by evaporation to achieve a concentration of 350 g.l⁻¹. To achieve an industrial grade product, two serial crystallizations are required. Crystals are formed using a cooling crystallizer at 15 °C. The solid material is separated later and the waste liquor, which still has a high concentration of IA, is sent back to the evaporator in order to be concentrated again and repeat the steps of crystallization.

The crude crystals can be purified using an active carbon treatment at 80 °C. This step aims to remove solid waste derived from fermentation. Subsequently, the treated broth is concentrated by evaporation and recrystallized. The crystals are separated from the liquid phase, which returns to the steps of concentration-crystallization while the crystals are dried, packed and sent for commercialization with high purity (99%).

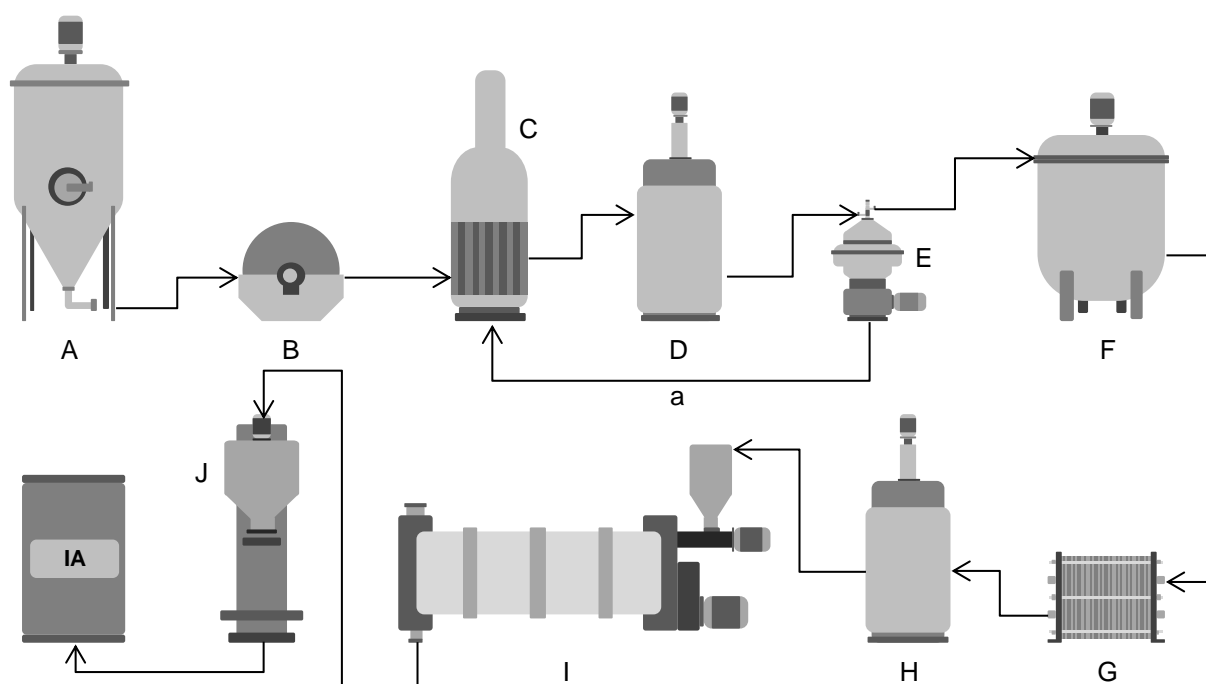


FIGURE 2.3. Schematic diagram of IA recovery process from fermentative broth (OKABE, 2009)
 A^ABioreactor; B^BFilter; C^CEvaporator; D^DCrystallization; E^ESeparator; F^FDecolorization; G^GHeat exchange; H^HRecrystallization; I^IDrying shelves; J^JPackaging; a^aSecond Crystallization

Dwiarti et al. (2007) purified IA using crystallization methods from two fermentation broths of hydrolyzed sago starch and glucose. A purity of 99.0% and 97.2%, respectively, for sago starch and glucose were reached at the end of purification. The melting points of the products were 166-169°C and 166-167°C, respectively. The IA purification by crystallization methods was successful, although the recovery yield was below the industrial model described by Okabe et al. (2009). TABLE 2.1 shows a comparison of experimental data using sago starch fermented with the industrial processed IA data according to Okabe et al. (2009).

TABLE 2.1. Recovery yields of IA (%) in specific downstream steps described in literature

Downstream step	Hydrolyzed Sago Starch ^a	Industrial Model ^b
Filtration	91.7	95.0
Concentration	84.8	93.1
Crystallization	51.3	74.5
Final Purity (%)	97.2	99.0

^aDWIARTI et al. (2007); ^bOKABE et al. (2009)

The waste liquor from the crystallizers is dark and supersaturated with residual IA. Zhang et al. (2009) observed that the addition of a small amount of pure IA crystals could destabilize the supersaturated system and recover 22.5g.l⁻¹ of IA from waste liquor with 169g.l⁻¹ of IA and 32.3mg.l⁻¹ of glucose. Change in suspension pH, temperature, or addition of activated carbon cannot destabilize the supersaturated system. The presence of glucose enhances IA crystallization from its solution prepared with pure water. Conversely, the presence of residual glucose in the waste liquor interferes with the IA crystallization.

2.4.2. Precipitation

IA can be recovered by precipitation with lead salts. This precipitate is filtered and then separated from the liquid-phase. The lead itaconate salts can be regenerated by adding carbonate or bicarbonate of alkali metals or ammonium to obtain the respective itaconate salts and lead carbonate. Subsequently, to isolate IA it is necessary to use a cation exchange step. The generated carbonate can be recovered and reused in new precipitations (KOBAYASHI and NAKAMURA, 1971). Another IA precipitation method uses calcium hydroxide. In this method, calcium itaconate precipitate is formed and recovered by filtration. The IA can be converted by reacting with sulfuric acid and purified using activated carbon and crystallization. However, this recovery method produces a large amount of calcium sulfate sludge as waste (WASEWAR et al., 2011b).

2.4.3. Liquid-Liquid Extraction

The extraction using organic solvents is one of the possible methods for IA recovery. The use of conventional solvents, such as long chain alcohols, esters and alkanes is not effective for the recovery of organic acids due to the low distribution coefficient of the acid, i.e., its higher solubility in water than in organic solvents (WASEWAR et al., 2011a; KAUR and ELST, 2014). However, the distribution coefficient may be altered by the use of reactive extraction, where the acid-extractant complex formed has a strong affinity for the organic phase (a solvent called diluent in this kind of extraction). The acid may be recovered from this complex and thereby the extractant can be regenerated to be used again in another extraction. Reactive extraction has been widely used and has provided improved results in the recovery of organic acids with selected extractants and diluents (KAUR and ELST, 2014).

Organophosphates and aliphatic amines have been studied as extractants for the separation of IA from aqueous phase due to their thermal stability and their ease of regeneration, which can be done by simple distillation (HANO et al., 1990; BRESSLER and BRAUN, 1990; MATSUMOTO et al., 2001; WASEWAR et al., 2011a; WASEWAR et al., 2011b; ASÇI and INCI, 2012; KAUR and ELST, 2014). However, studies made by Matsumoto et al. (2001) demonstrated that tri-n-octylamine (TOA), a long-chain aliphatic amine, is more effective in the reactive extraction processes of IA than tri-n-butylphosphate (TPB), an organophosphate, using hexane as diluent. Various kinds of aliphatic amines may be used as IA extractants. According to Bressler and Braun (1990), the extraction in aqueous phase has been improved in the order quaternary ammonium > tertiary > secondary > primary amines in 1-octanol and dichloromethane (DCM). The reactive extraction of IA using a quaternary ammonium, methyl tricapryl ammonium chloride (Aliquat 336), in different diluents was studied by Wasewar (2011b). Among diluents tested, ethyl acetate (an ester) enhanced significantly the extraction of IA in the organic phase when compared with kerosene (an aliphatic hydrocarbon mixture), toluene (an aromatic hydrocarbon) and hexane (an alkane). Kaur and Elst (2014) analyzed the reactive extraction of IA based on an investigation of eight different extractants in various combinations with seventeen types of diluents consisting of alcohols, esters and alkanes. The systems formed by trioctylamine, dioctylamine and N-

methyldioctylamine extractants dissolved in 1-octanol (an alcohol), pentylacetate and methyloctanoate (both esters) were found to be the most suitable.

The key point in the development of a reactive extraction system for the recovery of organic acids produced from bioreactors is the integration of bioprocess and recovery units. A problem of using these systems is the toxicity of components. Therefore, the selection of extractants and diluents that cause the minimum toxicity and maximum capacity in process is essential. Studies of toxicity in reactive extraction were done by Wasewar et al. (2011a), who had success in using a non-toxic diluent, sunflower oil, with a quaternary amine extractant, Aliquat 336.

IA can be regenerated from the loaded organic phase using back-extraction methods. There are different techniques for back-extraction of the acid-laden organic phase, such as temperature and diluent swing, using sodium hydroxide (NaOH), hydrochloric acid (HCl) solution or trimethyl amine (TMA). Poole and King (1991) investigated the back-extraction using a TMA, a stronger volatile tertiary amine, in aqueous phase. TMA is in contact with the loaded organic phase and forms a complex with the acid that can be regenerated in a subsequent step by evaporation of the amine. Keshav and Wasewar (2010) investigated the back-extraction of propionic acid from the loaded organic phase using different techniques of regeneration. Using such techniques with NaOH and TMA, the acid recovery can reach 100%, and TMA can be easily recycled by application of heat due to its volatility.

2.4.4. Electrodialysis

IA can be separated in a straightforward way from the fermented broth by electrodialysis. This is a unit operation of separation or concentration of ions in solutions consisting in the application of an electric field, forcing the ions transference through anion exchange membranes. Thus, IA can be separated from the other uncharged components of the fermentation broth, such as the residual glucose. This process does not require the use of heat or toxic additives. Electrodialysis has the potential to allow the fermentation and the continuous removal of IA, which may be used simultaneously with the control of the pH of the fermenter.

The transport of the ions through solution and membranes is caused by the electrical potential established by electrodes during electrodialysis. The resistance to chemical species transport relies on ionic charge and distribution activity. Due to its two carboxylic groups, IA may be present as three different species depending on the pH of the solution. Therefore, it is necessary to work in a pH around the second pKa of IA, where the acid is fully ionized and the solution is highly conductive. Stodollick et al. (2014) investigated a short-cut model to quantify the electric resistance of the concentration boundary layer and anion exchange membrane at over limiting current density using electrodialysis with bipolar membranes (EDBM) for separating IA. This resistance follows an exponential law and depends on pH and ionic strength only with regards to the absolute level of the current. Fidaleo and Moresi (2010) modeled the recovery of IA through electrodialysis with univalent electrolytes converting the acid into a disodium salt. Itaconate anions were transported through the anion membrane with a solute yield of 98%.

2.4.5. Diafiltration

Diafiltration is a method of separation or removal of components present in a solution by means of permeable membranes and a concentration gradient. This separation process may use incorporated membranes in bioreactors for the continuous *in situ* product recovery (ISPR) on a concept called "reverse-flow diafiltration" (RFD) (CARSTENSEN et al., 2012).

The RFD process yields a product stream through a hydrophilic ultrafiltration hollow-fiber membrane immersed in the bioreactor. The flow direction is reversed periodically with a wash solution to prevent loss of performance. This solution also has the function of feeding the bioreactor to maintain a constant volume. Carstensen et al. (2013) obtained 100% recovery with pure IA solutions, but only 60% from fermentation broths of *Ustilago maydis* using RFD. This indicates that constituents of the fermentation broth adversely affect permeability and product recovery. Compared with tangential flow processes, the RFD process minimizes the hydromechanical stress that causes wear of the membrane and the risk of oxygen limitations.

2.4.6. Pertraction

Li et al. (2013) investigated ISPR using pertraction to extract IA from the fermented broth. The pertraction technique uses an organic solvent to extract the solute from the aqueous phase by a similar procedure to liquid-liquid extraction, however, the solvents are separated by a hydrophobic membrane. Using 2-methyl tetrahydrofuran (2m-THF) as the solvent, about 50% of IA was extracted from the ISPR in a pertraction module.

2.4.7. Adsorption

Adsorption is a process of widespread use in industrial applications for purification and separation. The operation consists of using an adsorbent (a solid with affinity for the desired solutes) to separate the organic acid, that can later be recovered by eluting the loaded bed, while other components of the solution flow through the system. There is a wide range of adsorbents for adsorption processes, such as alumina, activated carbon, silica, and several kinds of synthetic ion exchange resins. Gulicovski et al. (2008) found that the IA adsorption on the surface of alumina is extremely pH dependent, the maximum adsorption occurred at a pH value of the first dissociation constant, pK_{a1} .

2.5. CONCLUSIONS

The development of an efficient process for separating and purifying itaconic acid (IA) from fermentation broths face difficulties due to the high affinity of this hydrophilic solute for aqueous solutions and the complex composition of the fermentation broth. Crystallization not only requires a high input of energy, but also efficient removal of impurities. The separation by electrodialysis, diafiltration and pertraction gives low yields due to loss of product in the effluent. Furthermore, the

lifetime of the membranes may be relatively short due to hydromechanical wear. The "reverse-flow diafiltration" method may be the most promising way for membrane recovery methods due to decreased stress on the membrane. Reactive extraction need complicated pretreatment (removal of proteins, biomass and salts), plus a subsequent step of back-extraction. Moreover, the cost of extraction agents and their toxicity is an obstacle to the application of reactive extraction in large scale. The adsorption still needs to be further investigated to be compared with the studied methods (TABLE 2.2).

A major challenge for the successful separation of IA from fermentation broths is how to apply separation technology for industrial processes and lower the cost on a large scale effectively, while increasing productivity and revenue. From the above analysis, it is evident that there is a need for further studies to develop a process that ideally should be simple to perform and give high yields and purity for the IA from fermentation broths.

TABLE 2.2. Main process of IA recovery.

Method	IA Solution	Yield (%)	Reference
Crystallization	Fermented both	54	Dwiarti et al. (2007)
Reactive Extraction	Aqueous solution	98	Aşçi and Inci (2012)
Reactive Extraction	Aqueous solution	97	Kaur and Elst (2014)
Reactive Extraction	Aqueous solution	65	Wassewar et al. (2011)
Reactive Extraction	Aqueous solution	80	Wassewar et al. (2010)
Electrodialysis	Aqueous solution	98	Fidaleo and Moresi (2010)
Diafiltration	Aqueous solution	100	Carstensen et al. (2013)
Diafiltration	Fermented both	60	Carstensen et al. (2013)
Pertraction + Extraction	Fermented both	50	Li et al. (2013)

3. SPECTROPHOTOMETRIC METHOD FOR DETERMINING ITACONIC ACID BY COMPLEXATION WITH TRANSITION METALS

3.1. ABSTRACT

The simple determination of itaconic acid (IA) in aqueous solutions is essential for monitoring bioproduction and for screening new microorganisms capable of producing this promising bio-building block. IA is capable of complexing cations, and we found that some of the corresponding complexes have absorption spectra sufficiently different from that of the separated components, allowing indirect determination of IA through a simple, two-step spectrophotometric analysis. Transition metal cations were selected based on the analysis of their absorbance spectra in aqueous solution, with and without itaconic acid. Metals that showed the highest absorbance were copper (at 745nm), nickel (at 395nm) and cobalt (at 520nm). The most promising metal for developing a determination method of itaconic acid was copper (II), because of higher intensity reading in complexed form. The appropriate concentration to read absorbance for copper was 20mM. However, there is a high influence of pH on the formation of complexes, and the observed shift in wavelength maxima is too small for analysis

3.2. INTRODUCTION

Good analytical methods are essential for the development of bioprocesses. However, the most sensitive methods are not always accessible for a laboratory or industry, or not suitable for high throughput analyses – e.g. for culture media optimization. In such cases, reviving old wet-chemistry techniques may prove useful, for several samples may be processed in parallel, reducing overall analysis times. This is what we needed for determining culture ideal conditions for cultivation of *Aspergillus terreus*, for the development of a process for production of itaconic acid (IA).

The determination of IA is usually done by high-performance liquid chromatography, HPLC. However, there are other quantitative methods such as titration with bromide in the fermented broth (FRIEDKIN, 1945) and through the direct reaction of pyridine and acetic anhydride with IA (HARTFORD, 1962). These techniques use the specific characteristics of IA, namely its unsaturation, as a basis for the determination.

Another useful characteristic of IA is that it is a diacid. It was postulated that its anions could form complexes with transition metal ions, as happens with other acids such as citric or EDTA. If IA complexes were formed, there could be a detectable shift in the absorption wavelength or intensity in the UV-VIS region in comparison with the free ions. Therefore, the formation of complexes using several potential cations was evaluated.

Several transition metals in aqueous solution are capable of forming complexes with water molecules through a dative or coordinate covalent bond. The cations work as an electron acceptor (Lewis acid) and water as an electron donor (Lewis base). Werner's theory explains the types of bonds in coordination complexes where the ions or molecules can behave as binders and transition metal ions can form complexes (LAWRANCE, 2010). According to Werner, there are two aspects: the primary is responsible for the charge number of the ion complex and the secondary is the coordination number of the compound. Binders having only one coordination site are called monodentate; those having more than one site are called polydentate chelators.

Organic acids can form coordinated bonds when their carboxyl groups are present deprotonated. Studies on the formation of copper complexes have been done with malic acid, itaconic acid (RAMAMOORTHY and SANTAPPA, 1963), citric acid and ethylenediamine tetraacetic acid (EDTA) (ZAKI and ALQASMI, 1981). This study sought to develop a colorimetric method for determining IA in aqueous solutions from spectrophotometric readings in visible light wavelengths.

3.3. MATERIALS AND METHODS

3.3.1. Selection of Transition Metals

Sodium itaconate was chosen for testing, in order to ensure eventual complex formation. The salt was prepared by neutralization, in a 2:1 molar proportion of sodium hydroxide and itaconic acid (denoted IA, Aldrich Company Co., $\geq 99\%$), respectively. This solution was concentrated using a rotary evaporator at 60°C , with pressure of 560mmHg, and then crystallized and dried at 80°C (FIGURE 3.1).

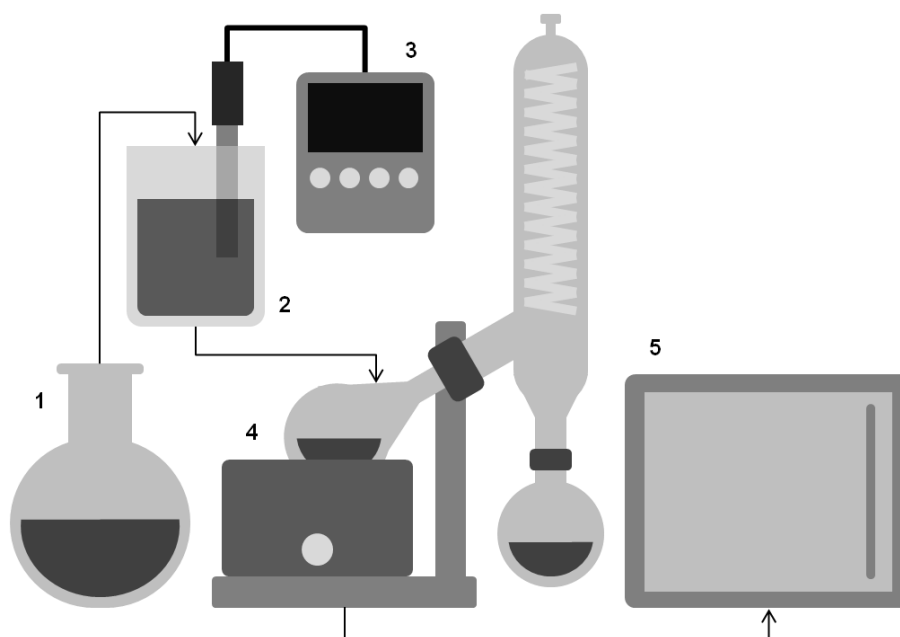


FIGURE 3.1. Schematic diagram for the preparation of the sodium itaconate salt (1) Sodium hydroxide; (2) itaconic acid; (3) pHmeter; (4) rotary evaporator; (5) incubator heating.

Several transition and non-transition metals were analyzed in order to select the potential complex formed with itaconate: aluminum sulfate, calcium chloride, potassium chloride, manganese sulfate, magnesium sulfate, cobalt chloride, copper chloride, nickel sulfate, iron sulfate (II) and iron chloride (III). The selection was made by evaluating the effect of the salts absorbance in the presence of sodium itaconate in the visible wavelength range (FIGURE 3.2). If there is no interaction, then the

absorbance of the mixture metal-itaconate should be the algebraic sum of each species absorbance in a certain wavelength. However, if a chelate is formed, the free metal concentration would be affected, and the obtained experimental absorbance would be different from the algebraic sum of absorbances.

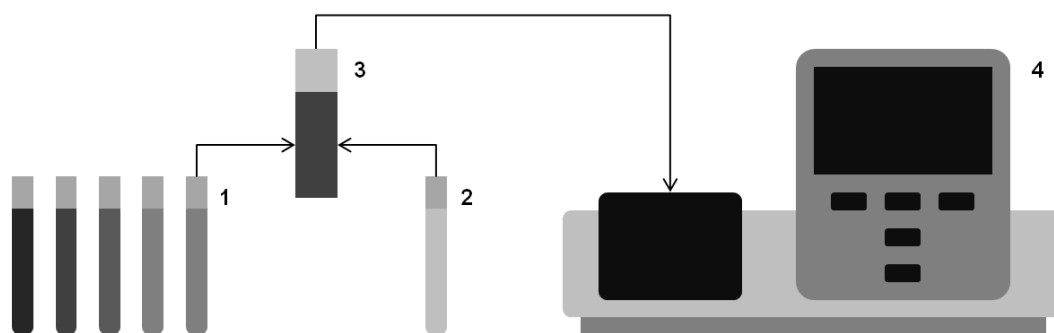


FIGURE 3.2. Schematic diagram for the spectrophotometric analysis for transition metal selection with potential complexation with itaconate

(1) Solutions of different transition metal salts; (2) sodium itaconate; (3) mixture metal-itaconate; (4) spectrophotometer

The spectra were read using a scanning spectrophotometer in a range encompassing the visible range and part of the UV and IR spectrum, from 300 to 1000nm, with aqueous solutions of each metal salt and for the mixture salt-itaconate, in concentrations of 10mM for every component. The proportion between absorbance and wavelength for the pure reagents were confronted with the ones for the metal-itaconate mixtures, using *Microsoft Excel 2013*, in order to detect differences that would be peculiar for a complex.

3.3.2. Job's Method

Job's method is a spectrophotometric method used to establish the stoichiometry of complex formed between of species pairs, usually an organic compound and a cation (RENNY et al., 2013). The method is based in the fact that maximum light absorption among free and complex forms can be correlated with the individual complex stoichiometry.

Different concentrations of the transition metals and itaconate were used. Despite the concentration being different, the sum of the molarities for each component was maintained, as showed in TABLE 3.1. Scanning spectra were made in order to determine the maximum absorbance of the selected metals. The Jobs Graphic was made based on the absorbance values for each separate component and for the mixture, in a determined concentration, according to the following equation:

$$Abs_{Job} = Abs_{complex} - Abs_{transition\ metal} - Abs_{itaconate}$$

TABLE 3.1. Concentration of transition metals and itaconate used to prepare Jobs Graphic

Proportion (mM:mM)	Complex		Pure solution	Pure solution
	Sodium itaconate (mM)	Transition metal (mM)	Sodium itaconate (mM)	Transition metal (mM)
0:60	0	60	0	60
10:50	10	50	10	50
20:40	20	40	20	40
30:30	30	30	30	30
40:20	40	20	40	20
50:10	50	10	50	10
60:0	60	0	60	0

3.3.3. pH Effect

To determine the pH effect in the itaconate complexation, essays with different pH values were done using sodium hydroxide and hydrochloric acid solutions. The pH has a direct influence on the concentration of the eventually formed complex in the presence of transition metal, because sodium itaconate may be present in solution in both reduced or deprotonated forms. FIGURE 3.3 represents the concentration and protonated forms in which the IA may be present depending on the pH. IA has three different states of protonation with dissociation constants in aqueous solutions of pK_{a1} (3.55) and pK_{a2} (5.55).

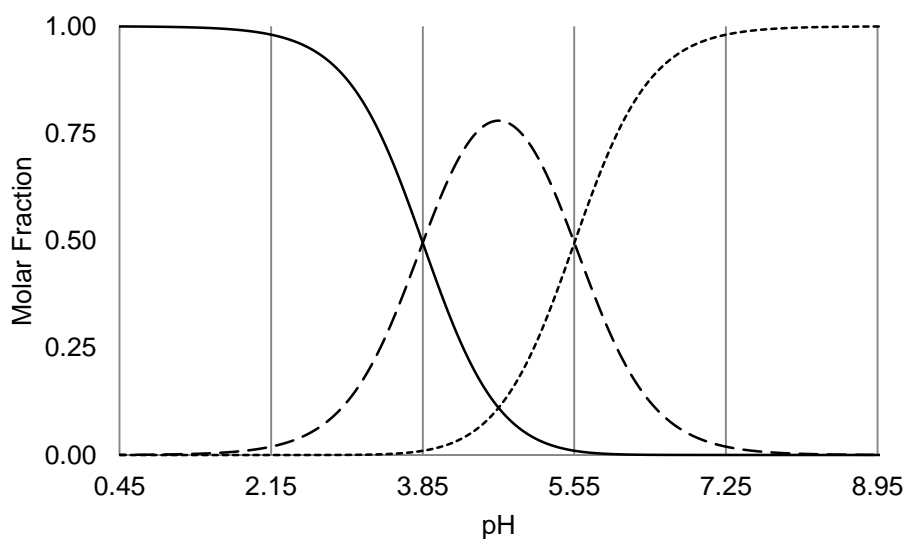


FIGURE 3.3. Effect of pH on the itaconic acid deprotonation
 (—) $C_3H_4(COOH)_2$; (---) $C_3H_4(COOH)(CO^-)$; (- - -) $C_3H_4(CO^-)_2$

The search for a buffer was performed to prevent the pH interference in the reading. However, copper is easily precipitated in alkaline media, preventing the use of various standard solutions, such as phosphate-based buffers. Other basic solutions as acetate and ammonia, despite forming salts with high solubility, affect reading by interfering in a possible bond between itaconate and copper. Therefore, the solution contained nitrate, a base with extremely high solubility with copper and that does not cause interference in reading complex. In order to determine the effect of copper concentration in the precipitation, tests were performed, using sodium nitrate, with various concentrations of the mixture of copper and itaconate (TABLE 3.2).

TABLE 3.2. Tests of the effect of copper concentration on the precipitation with itaconate

Assay	Sodium Itaconate (mM)	Copper Chloride (mM)	Sodium Nitrate (M)
A	20.00	20.00	1.00
B	30.00	30.00	1.00
C	40.00	40.00	1.00
D	50.00	50.00	1.00

3.4. RESULTS AND DISCUSSION

3.4.1. Selection of Transition Metals Showing Potential Complexation with Itaconate

The selection of the transition metals with the potential to form complex was performed by scanning spectrophotometer. Each component was separately read and compared with the spectrum generated from the mixture with sodium itaconate. The scans shown in FIGURE 3.4 indicated that the itaconate only presents significant absorbance at a wavelength below the ultraviolet (UV) light. Thus, the presence of itaconate should not contribute to increase the absorbance in the wavelength range tested.

Aluminum (II), calcium (II), potassium (I), manganese (II) and magnesium (II) readings did not present significant differences, i.e., the spectra generated by their respective salts had the same absorbance profile compared with their mixture with sodium itaconate. The iron (II) and iron (III) presented higher absorbance for the mixture compared to the pure solutions, but there was precipitation, and so, these metals should be used in very low concentrations. This low solubility would be detrimental in a possible method of determination, because of the low absorbance values, with a greater possibility of error in reading by the presence of contaminations.

The transition metals which had an increase in absorbance in the presence of itaconate were cobalt (II), nickel (II) and copper (II) with maximum intensity at wavelengths 520, 395 and 745nm, respectively. Therefore, these metals were selected as potential reagents for complexation with itaconate.

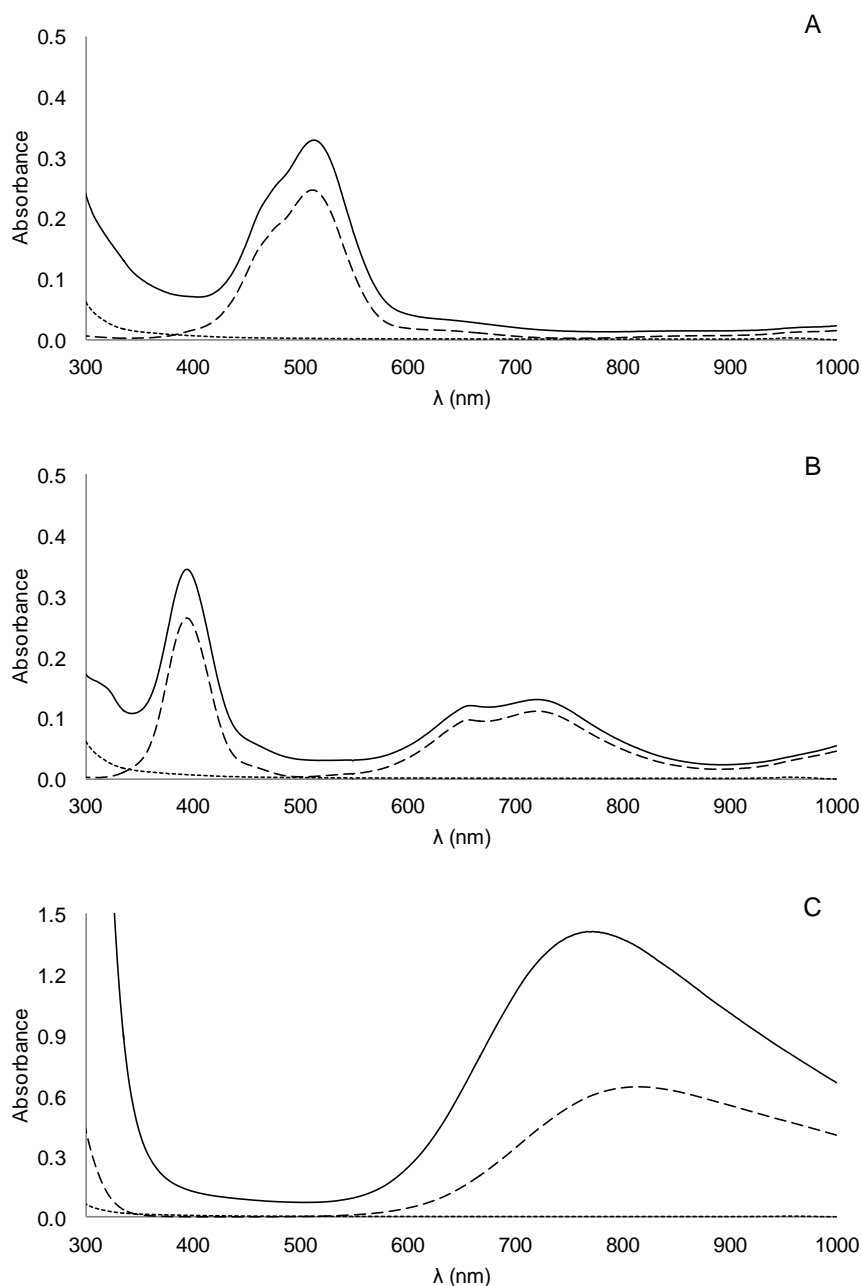


FIGURE 3.4. Effect of itaconate in the spectra of different transition metals in aqueous solution (A) Cobalt chloride; (B) nickel sulfate; (C) copper chloride; (- - -) sodium itaconate; (— —) transition metal salt; (—) mixed solutions

3.4.2. Determining of the Optimum Component Proportion for Each Complex

The next step after the selection of the most suitable metal for a possible complexation is determining how the proportion of each component interferes with the spectrophotometric reading methods. The Job's method allows the stoichiometric

definition of the components and also makes evident the complex formation. As sodium itaconate has no significant reading within the length of visible light, the increased concentration of the tested metals (0 to 60mM) would indicate an increase in the intensity of the absorbance, even with decreasing acid concentration (60 to 0mM). FIGURE 3.5 shows that the amount of cobalt is more significant to absorbance than itaconate or the mixture of both, especially in the wavelength region between 450 and 600nm.

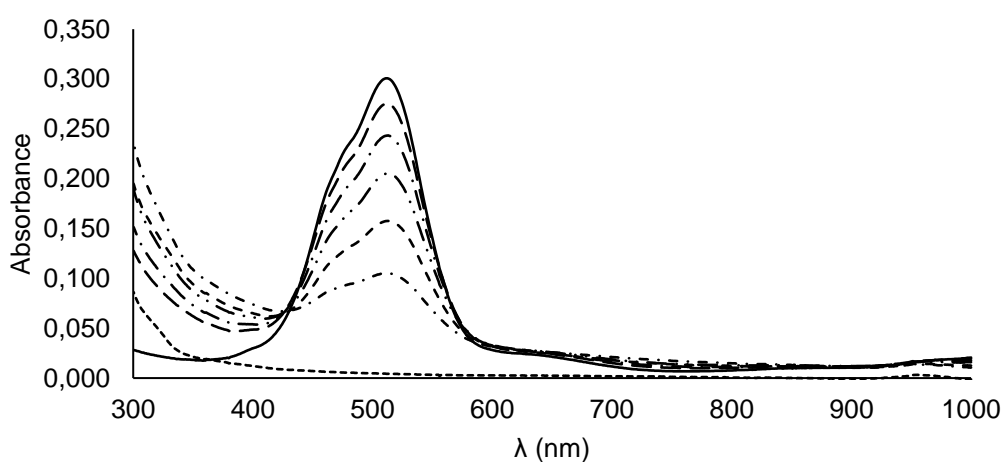


FIGURE 3.5. Absorbance spectra of solutions with different concentrations of sodium itaconate-cobalt chloride (mM:mM)
 (.....) 60:0; (- · -) 50:10; (- - -) 40:20; (- · ·) 30:30; (- · -) 20:40; (- - -) 10:50; (—) 0:60

When applying the Job's method, the proportions 30:30, 40:20 and 50:10 itaconate:cobalt provided similar absorbance intensities, as shown in FIGURE 3.6. Thus, more than one type of binding between molecules may be occurring simultaneously.

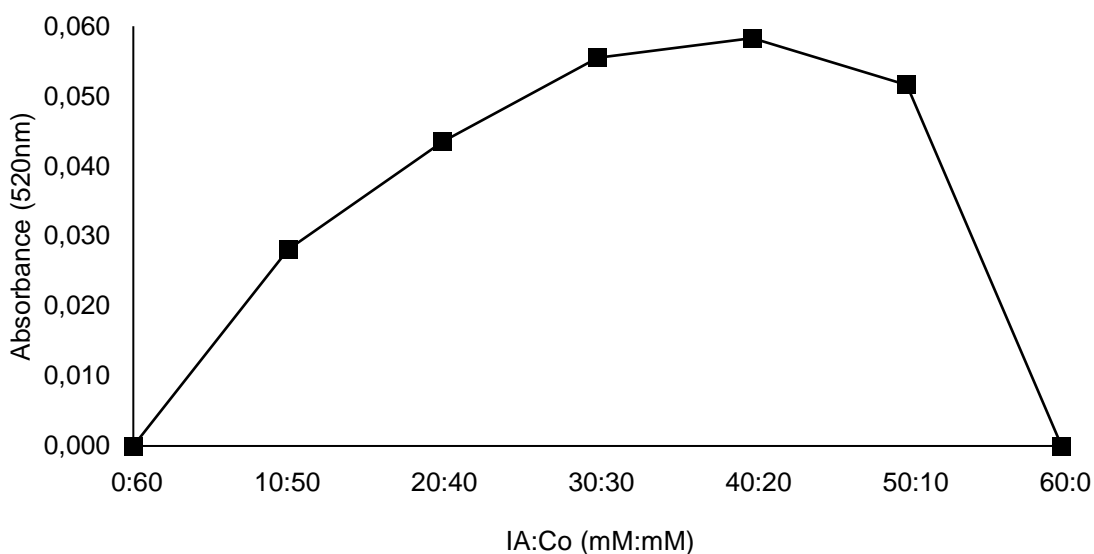


FIGURE 3.6. Job's method applied to different proportions of sodium itaconate and cobalt chloride

The same tests were performed for nickel, indicating two intensifications of absorbance at 400 and 700nm (FIGURE 3.7). As cobalt, nickel presented higher significance to rising absorbance than itaconate or the mixture.

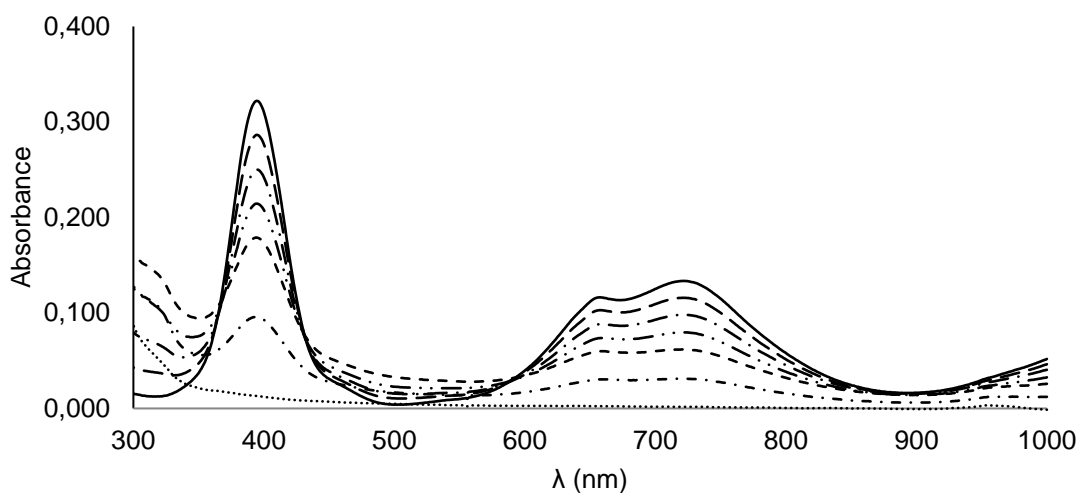


FIGURE 3.7. Absorbance spectra of solutions with different concentrations of sodium itaconate: nickel sulfate (mM:mM)
 (.....) 60:0; (- · - ·) 50:10; (- - - -) 40:20; (- · · ·) 30:30; (- · - -) 20:40; (- - - -) 10:50; (————) 0:60

Job's method indicated a nickel-itaconate ratio of 1:2, therefore, the proportions 0:60, 10:50, 20:40, 30:30, 40:20, 50:10 and 60:0 used to generate the graph of FIGURE 3.8 may be replaced by complex concentrations of 0, 5, 10, 15, 20,

10 and 0mM, respectively. A graph relating the absorbance and the complex concentration with a regression coefficient of 0.996 can be generated from these data.

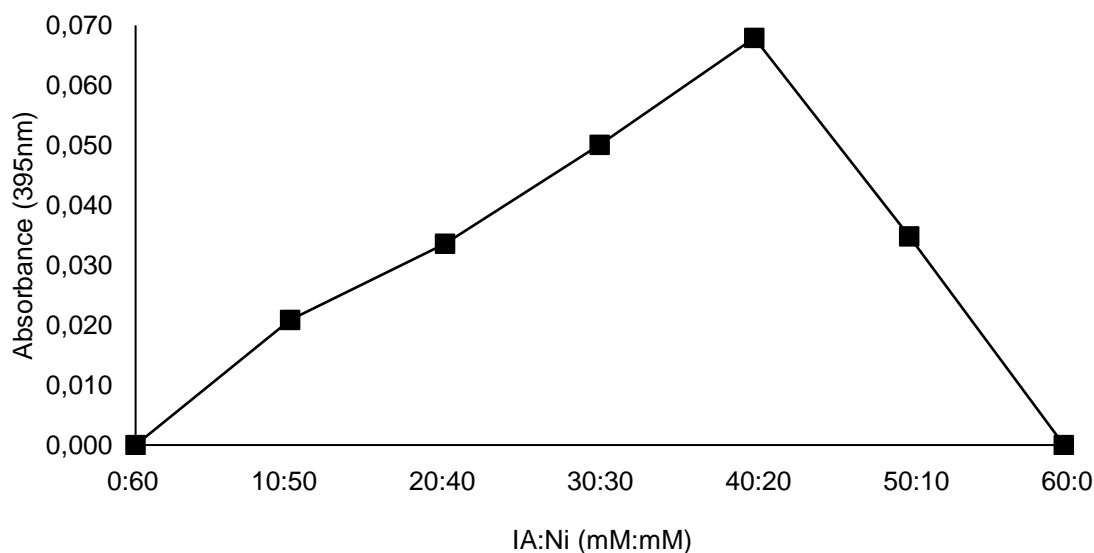


FIGURE 3.8. Job's method applied to different proportions of sodium itaconate and nickel sulfate

Copper was proved as the most suitable complex generator metal, as well as presented greater absorbance intensity than the other metals tested. It also had a greater significance for mixing with itaconate. FIGURE 3.9 shows that the concentrations of 30:30, 20:40 and 10:50 (mM:mM) itaconate:copper showed higher absorbance spectrum when compared with pure copper concentration of 60mM.

Job's method indicates a ratio of 1:1, i.e., the concentration of the complex is limited by both the copper and the itaconate. Replacing the data in FIGURE 3.10, one can generate a plot relating the absorbance and the concentration of the complex ranging from 0 to 30mM. A linear regression of the data generated provides a straight line with error coefficient of 0.938. This error can be reduced by removing the effect of pH, since copper is more sensitive than other metals and can easily be precipitated as copper hydroxide. Thus, it is necessary to further investigate the effect of pH on the formation of a metal complex.

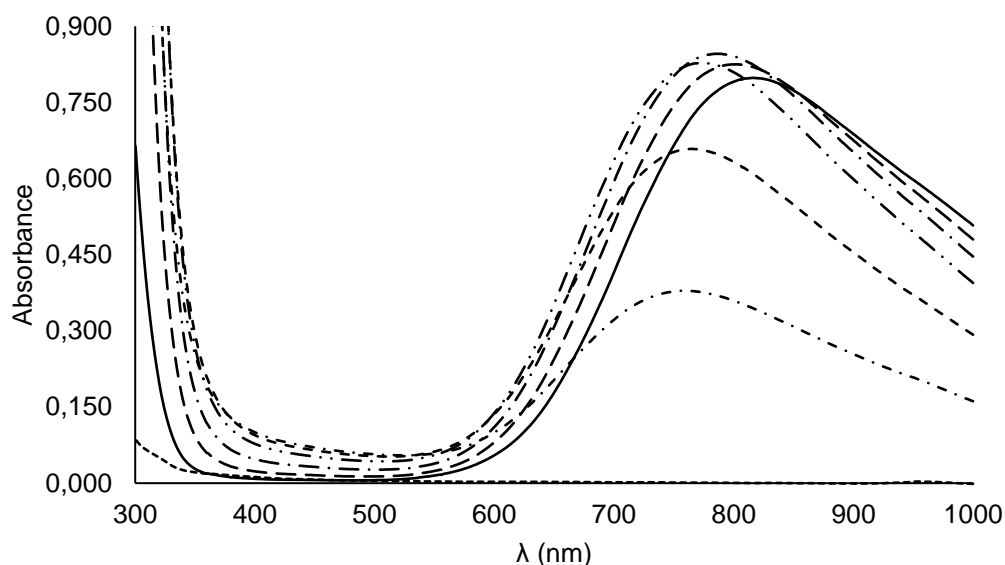


FIGURE 3.9. Absorbance spectra with different concentrations of sodium itaconate/ copper chloride (mM:mM)
 (.....) 60:0; (- · -) 50:10; (- - -) 40:20; (- · ·) 30:30; (- · -) 20:40; (- - -) 10:50; (—) 0:60

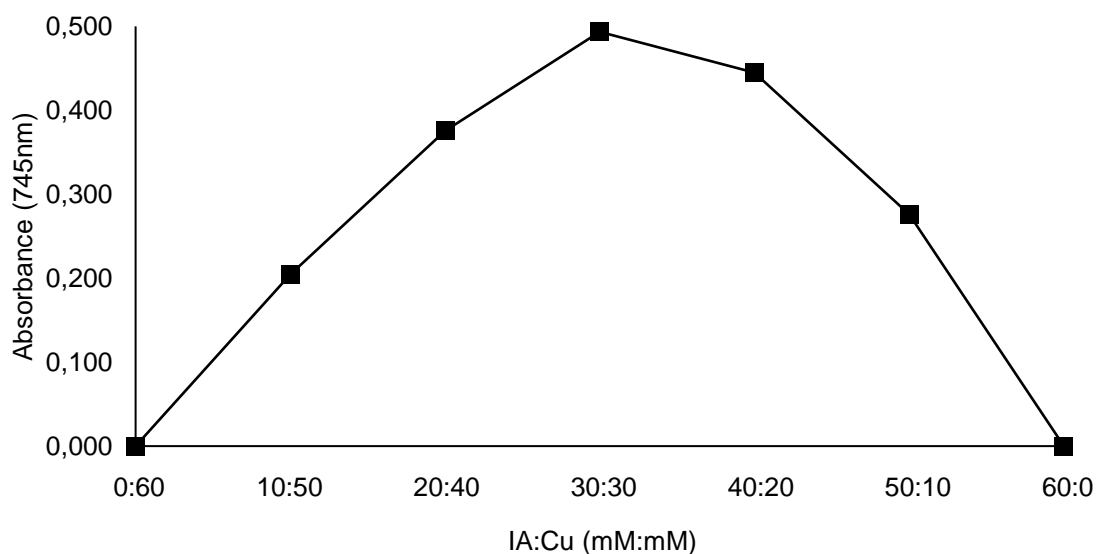


FIGURE 3.10. Job's method applied to different proportions of sodium itaconate and copper chloride

3.4.3. Effect of pH on the Absorbance of the Complex

The copper (II) was the transition metal with more significant results for complex formation with itaconate. However, factors such as pH can cause errors in spectrophotometer reading, for copper can suffer precipitation with strong bases, and itaconate can be reduced in its acid form or deprotonated in its ionic form. The effect

of pH on the absorbance of the copper solution (10mM) did not show significant variations in reading within the pH range examined (2.5 to 4.0). However, the metal itaconate spectrum results were quite different for the pH range (2.8 to 5.3) and can be analyzed in FIGURE 3.11.

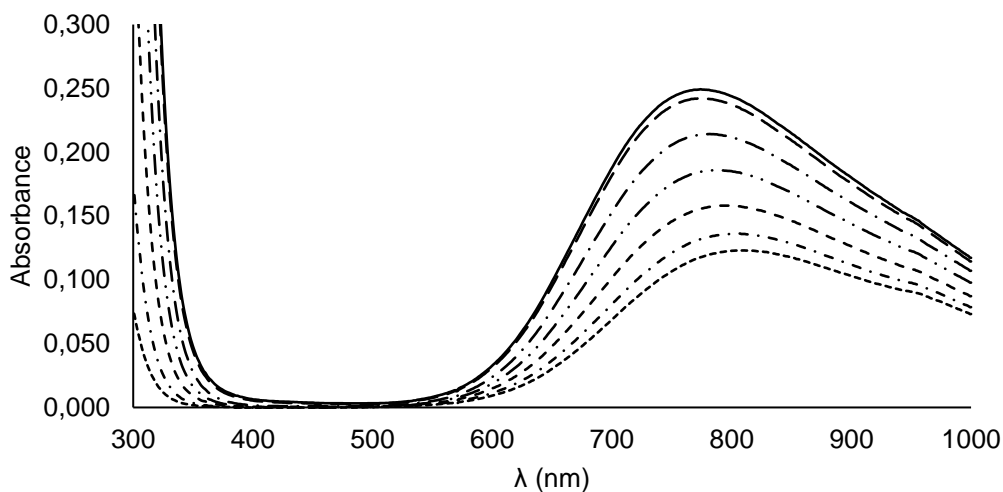


FIGURE 3.11. Effect of different pH in the absorbance spectra of sodium itaconate-chloride copper (.....) 2.76; (- · -) 3.16; (- - -) 3.65; (- · ·) 4.05; (- · -) 4.52; (- - -) 5.15; (—) 5.29

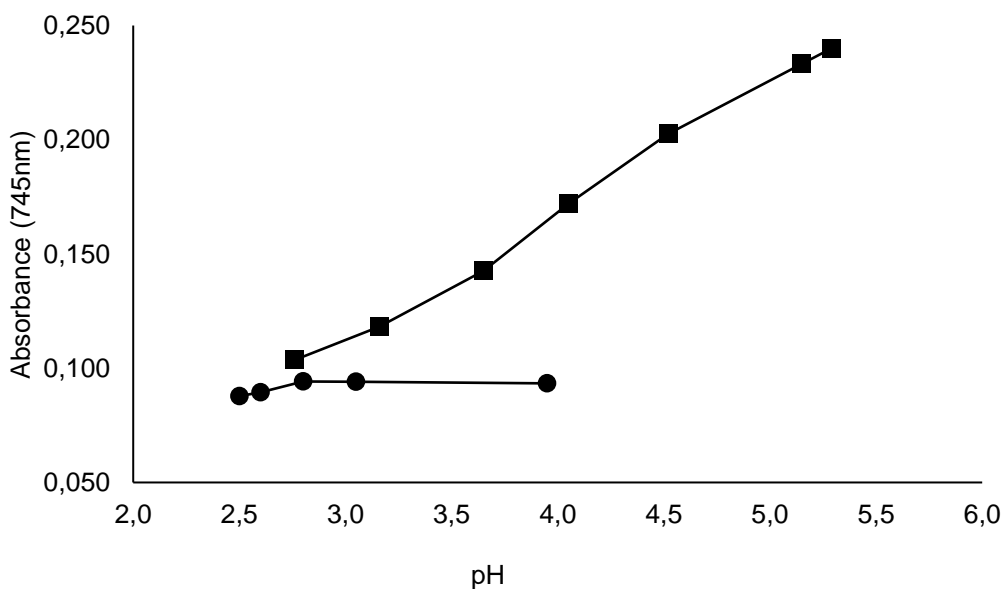


FIGURE 3.12. Effect of different pH in copper-itaconate complex and copper in presence of chloride (■) copper-itaconate (10mM); (●) copper chloride (10mM)

The increase in absorbance intensity between 600 and 1000nm may be explained by deprotonation of IA. The increase in pH caused the formation of more itaconate molecules which may indicate that the higher the deprotonation, higher the possibility of complexes formation. The graph shown in FIGURE 3.12 indicates that there is a greater interference of pH on the absorbance of the mixture itaconate-copper and an insignificant difference for copper.

Using sodium nitrate (1M), tests were performed with various concentrations of the mixture of copper (II) and itaconate (10, 20, 30, 40 and 50mM) to evaluate the effect of precipitation. The results presented in FIGURE 3.13 showed no precipitation at a concentration of 20mM after 48h of reaction.

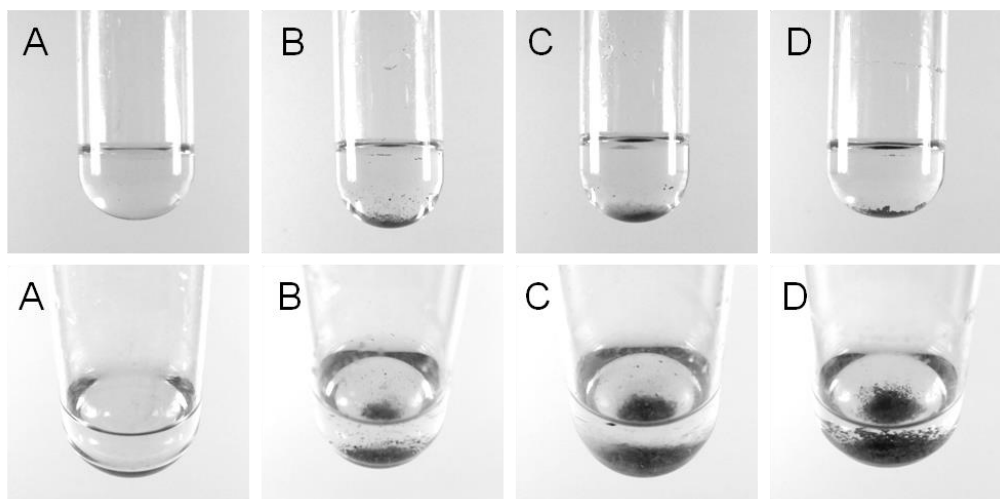


FIGURE 3.13. Effect of concentration of mix on the precipitation
(A) 20; (B) 30; (C) 40; (D) 50mM

3.4.4. Determination of the Concentration Curve

After choosing the condition for maintaining the pH at appropriate levels of balance, it was possible to apply the readout method using sodium nitrate as a buffer solution. The reading with different concentrations of itaconate (0 to 10mM) and copper (20mM) using nitrate solution as buffer allowed determining the absorption coefficient for different combination as presented in TABLE 3.3. The graph of absorbance read at 745nm with respect to the concentration of a straight itaconate

enable the generation of a linear regression coefficient of 0.999 (FIGURE 3.14). Thus, one can determine the concentration of itaconate with an absorptivity coefficient of 63.3mM. The mixes solution of copper, itaconate and nitrate kept stable at pH 4.86 ± 0.05 , even by varying the concentration of itaconate (0 to 10mM).

TABLE 3.3. Determination of the concentration curve of itaconate

Itaconate (mM)	Chloride Copper (mM)	Sodium Nitrate (M)	pH	Abs (745nm)
0.00	20.00	1.00	4.78 ± 0.02	0.246 ± 0.001
2.00	20.00	1.00	4.83 ± 0.02	0.280 ± 0.001
4.00	20.00	1.00	4.86 ± 0.01	0.312 ± 0.002
6.00	20.00	1.00	4.90 ± 0.01	0.345 ± 0.002
8.00	20.00	1.00	4.89 ± 0.01	0.374 ± 0.002
10.00	20.00	1.00	4.91 ± 0.01	0.404 ± 0.002

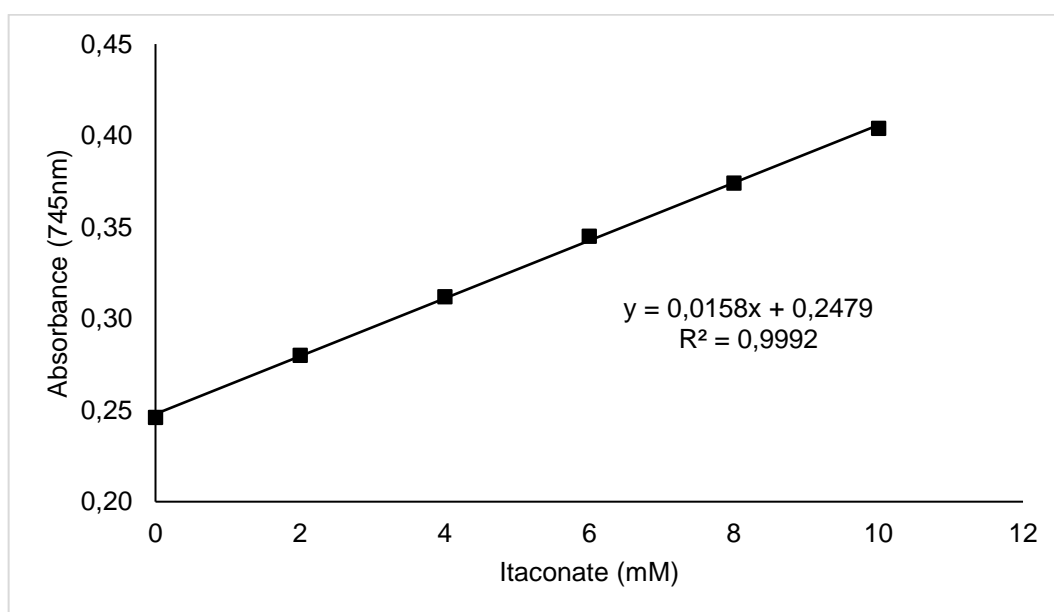


FIGURE 3.14. Concentration curve of itaconate.

3.5. CONCLUSIONS

The complexes formation with itaconate in the presence of transition metals could be confirmed with cobalt (II), nickel (II) and copper (II). However, the development of a method based on the formation of complexes with absorbance distinct from that of the components, essential to quantify the concentration of

itaconate, was elusive, mostly because of errors due to small-angle curves developed from the absorbance-concentration curves. Good results were achieved in the complexation of itaconate with copper. However, problems such as metal precipitation and deprotonation of the acid occurred. Sodium nitrate was found to be the best solution for pH stabilization. It was discovered that best conditions for determining itaconate (0 to 10mM) in aqueous solution were using copper (20mM) and nitrate (1M) and reading the absorbance at 745nm.

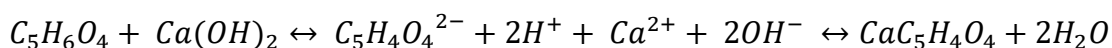
4. PRECIPITATION OF CALCIUM ITACONATE AND DETERMINATION OF ITS SOLUBILITY AT DIFFERENT TEMPERATURES

4.1. ABSTRACT

The search for processes for the recovery of organic acids with efficiency and low cost is one of the key steps for replacing petrochemical-based products. Despite advances in biotechnology in front of fermentation processes, the main bottleneck is still the separation and purification. Although the downstream of fermentation products in general, and of organic acids in particular is well developed, the studies on the precipitation of Itaconic acid (IA) are hardly found. This information is essential for process development. One of the most common separation methods for organic acids involves the precipitation and regeneration. In this study, the data for calcium itaconate solubility were determined in order to assess the potential precipitation of IA as calcium salt from the fermentation broth. The recovery demonstrated to be temperature-dependent and was of 88 to 97% in the range of 20 to 80°C. The regeneration of the acid with sulfuric acid was also evaluated, showing a recovery yield of 99%.

4.2. INTRODUCTION

Calcium itaconate ($\text{CaC}_5\text{H}_4\text{O}_4$) is a salt prepared by neutralization of Itaconic acid (IA) by calcium hydroxide $\text{Ca}(\text{OH})_2$, and is an important intermediate in the recovery stage of IA from the fermented broth by precipitation (KOBAYASHI and NAKAMURA, 1971). Soluble IA is converted into an insoluble itaconate by neutralization, as follows:



The precipitation occurs due to the low solubility of calcium itaconate, even if IA has water solubility between 70 and 80 g.l⁻¹ at 20°C (for a solubility-temperature graphic, check FIGURE 2.2). The low solubility of calcium itaconate may be used for the separation of IA as a solid precipitate, directly from clarified broths.

Calcium hydroxide also has a relatively low solubility, as described in FIGURE 4.1 (PERELYGIN et al., 2000). According to the graphic, the higher the temperature, the lower the solubility, which follows a straight line in the range from 20 to 80°C.

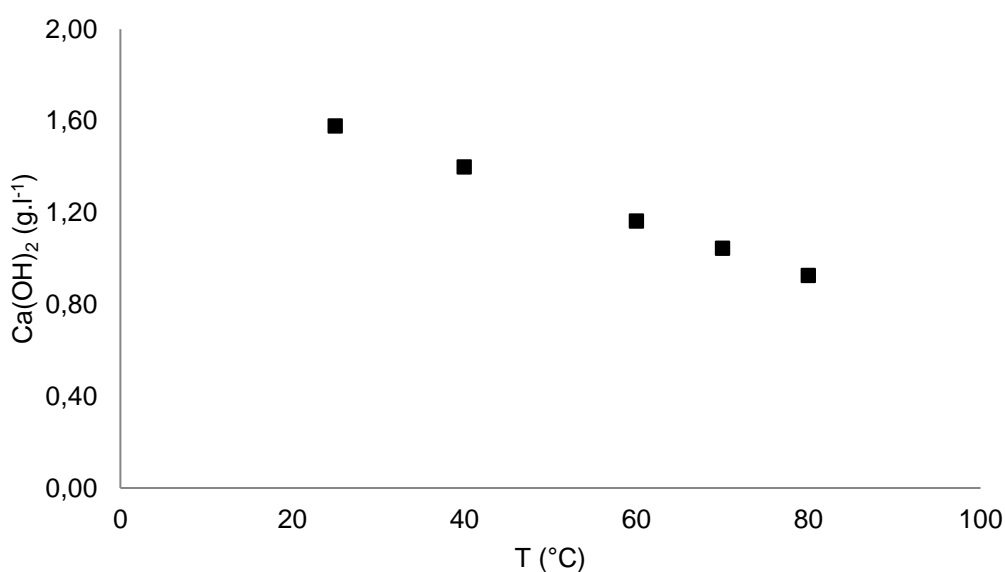


FIGURE 4.1. Effect of temperature on the solubility of calcium hydroxide in water

Although calcium itaconate is described as an intermediary in certain production technologies, data about its solubility are scarce. It is important to evaluate the solubility for recovery and crystallization of fermented IA, in order to define suitable conditions for downstream.

Therefore, this research aimed to determine the solubility of calcium itaconate through its precipitation from itaconate solutions, by stoichiometric neutralization with calcium hydroxide, followed by a gravimetric analysis. Redissolution of the salt produced was also evaluated in order to back-check the values obtained by precipitation.

4.3. MATERIAL AND METHODS

4.3.1. Preparation and Recovery of Calcium Itaconate

The salt was prepared by neutralizing in 1:1 molar ratio of calcium hydroxide and itaconic acid (denoted IA, Aldrich Company Co., $\geq 99\%$), respectively. The suspension formed was filtered to remove calcium hydroxide excess and its pH was adjusted with calcium hydroxide. The solution was again filtered and its pH was adjusted to 7.0. This solution was concentrated using a rotary evaporator at 60°C with the pressure of 560mmHg, crystallized and dried at 80°C (FIGURE 4.2).

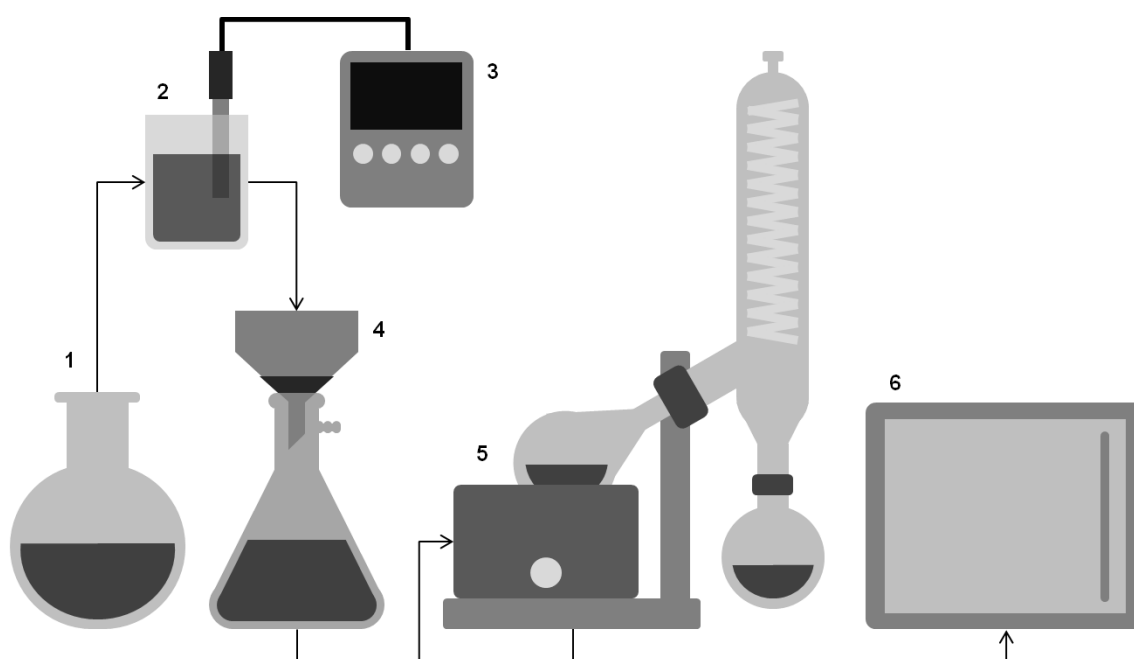


FIGURE 4.2. Schematic diagram for the preparation of the calcium itaconate salt (1) calcium hydroxide; (2) IA; (3) pHmeter; (4) filtration system; (5) rotary evaporator; (6) incubator

4.3.2. Determination of Itaconate Concentration by Spectrophotometry

To quantify the concentration of soluble calcium itaconate, absorption spectra were determined with a spectrophotometer with different concentrations of IA (0 to 10mM) between the wavelengths of 200 and 300nm. The phosphate buffer solution was used to stabilize the pH at 6.57 ± 0.07 . These curves were used for analysis, considering higher coefficient of regression for absorption x concentration.

4.3.3. Determination of the Solubility of Calcium Itaconate

The determination of the solubility of calcium itaconate in water was done with a mass of 0.5g of salt in 5.0ml of deionized water at different temperatures (10, 30, 50, 70 and 90°C) in test tubes for 60 minutes, and manually agitated every 15min. All assays were done in triplicate. After solubilization, the samples were kept at constant temperature for 60 minutes to ensure the precipitation of suspended calcium itaconate. The solubility was determined spectrophotometrically by removing an aliquot of 1.0ml of each test and reading its absorption using a previously determined equation for itaconate concentration x absorbance (FIGURE 4.3).

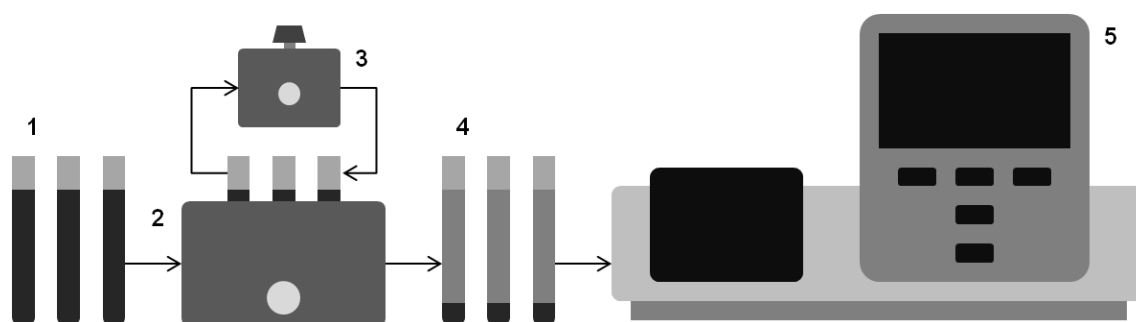


FIGURE 4.3. Schematic diagram for the determination of the solubility of calcium itaconate (1) calcium itaconate supersaturated solution; (2) thermal control; (3) vortex agitated; (4) calcium itaconate precipitated solution; (5) spectrophotometer

4.3.4. Regeneration of IA from Its Calcium Salt

The regeneration of IA was done by adding different concentrations of sulfuric acid (range 0 to 100mM) to 500 mg of calcium itaconate. The sulfuric acid was chosen to react with calcium itaconate forming calcium sulfate, which has low solubility in water, 2.4 g.l⁻¹ at 20°C (BOUIS, 2006). Assays were carried out at a temperature of 25°C for 60min with manual agitation every 15min, followed by precipitation for 60min. The same spectrophotometric method described in item 4.3.3 was employed to determine the concentration of soluble IA in this step.

4.4. RESULTS AND DISCUSSION

4.4.1. Determination of Concentration Curves for Itaconate by Spectrophotometric Method

IA is an unsaturated compound, which has a moderate absorbance in the UV range. This can be used for the determination of its concentration when the other components of the culture medium have low absorbance, as is the case for Ca²⁺, water, and SO₄²⁻.

The curves of scanning spectrophotometry for different concentrations of itaconate showed different peaks between 210 and 240nm, a shift possibly due to the presence of colloidal material. The curves are shown in FIGURE 4.4. However, when the data is processed into an absorbance-concentration curve, there is linearity and good correlation (0.99) between 230 and 250nm (FIGURE 4.5). Beyond the wavelength of 270nm, itaconate did not provide a high enough reading for a quantitative analysis method.

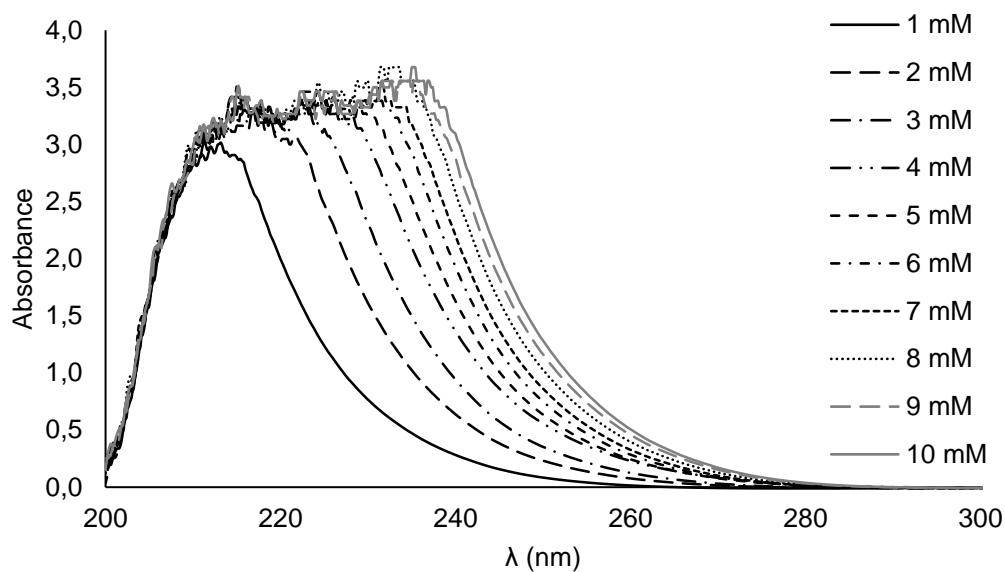


FIGURE 4.4. UV spectra of itaconate at several concentrations

The wavelength of 210nm was found to be ideal for analysis in the presence of low concentrations of itaconate. However, the curves generated in this wavelength did not show the good linearity necessary for a quantitative model, which was the focus of this experiment. Thus, to determine the concentration of itaconate from absorbance reading, the curve generated from readings at 240nm was used.

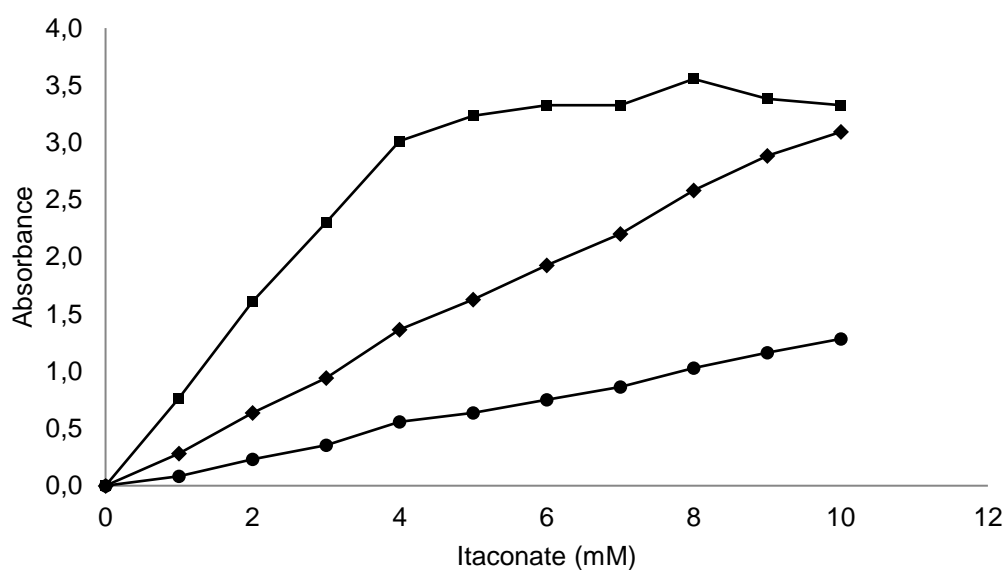


FIGURE 4.5. UV Absorbance of itaconate as a function of concentration
 (■) 230; (◆) 240; (●) 250nm

Following the law of Lambert-Beer, it is possible to determine the absorptivity of itaconate at the wavelength of 240nm:

$$Abs = \varepsilon \left(\frac{l}{g \cdot cm} \right) \times C \left(\frac{g}{l} \right) \times L(cm) \quad (1)$$

where *Abs* is absorbance at a certain wavelength, ε is absorption coefficient, *C* is the concentration of solute and *L* is the wavelength that light travels through the body width of the bucket (1cm).

Equation (2) is the result of the linear regression from the absorbance curve at 240nm, which can be seen in FIGURE 4.5. This equation can give us absorptivity (3):

$$Abs(240nm) = 3.14 \times C_{itaconate}(mM) \times 1cm \quad (2)$$

$$\varepsilon(240nm) = 3.14mM^{-1}cm^{-1} \quad (3)$$

Thus, to determine the concentration of soluble itaconate in this study the absorbance at 240 nm was read and converted into concentration in mM using equation (2).

4.4.2. Solubility of Calcium Itaconate

The solubility of calcium itaconate ranges from 10 to 17g.l⁻¹ in the temperature range between 10 to 90°C (TABLE 4.1). This is much lower than the solubility of IA, and also shows an inverse dependence with temperature – which is beneficial for its recovery from concentrated solutions of IA. These data are presented in FIGURE 4.6 where it can be seen that as temperature is increased, the solubility of calcium itaconate decreases. From in industrial processes, where there is IA concentration followed by precipitation, IA can be concentrated up to 350g.l⁻¹ by evaporating the water at 80°C; if calcium itaconate is precipitated at the same temperature, it is possible to recover about 97% of IA, showing it to be an efficient recovery strategy.

However, the fermentation broth contains other components that may be precipitated along with itaconate, so that purification of the regenerated acid is still necessary.

TABLE 4.1. Solubility of calcium itaconate at different temperatures

T (°C)	Calcium Itaconate (g.l ⁻¹)
10	17.282 ± 0.284
30	15.241 ± 0.529
50	13.293 ± 0.289
70	10.058 ± 1.052
90	10.312 ± 0.141

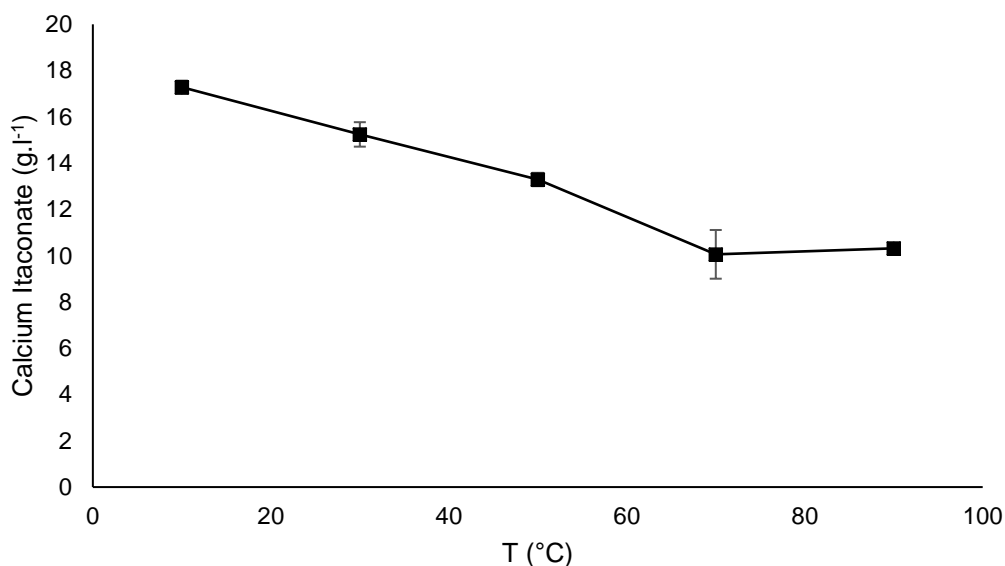


FIGURE 4.6. Solubility of calcium itaconate at different temperatures

4.4.3. IA Regeneration

The results of the dissolution tests shown in TABLE 4.2 demonstrate that the regeneration of IA is pH dependent. A concentration of sulfuric acid in a ratio of approximately 2.6 mol.mol⁻¹ IA/H₂SO₄ is sufficient for IA recovery. The recovery was 99.07% when 100mM of the acid was added. In FIGURE 4.7, it can be considered that the effect of the itaconate concentration is linear. Thus, one can conclude that the IA can be recovered by adding sulfuric acid, which can be separated by simple

filtration. However, this method generates calcium sulfate as a by-product, which is difficult to recycle because it is a low-solubility salt.

TABLE 4.2. Test results of the dissolution of itaconate with sulfuric acid at different concentrations

H ₂ SO ₄ (mM)	Itaconate (g.l ⁻¹)	pH	Yield (%)
0.000	15.435	7.02	30.70
10.035	19.718	5.55	39.34
19.863	23.388	5.20	46.31
29.919	26.824	5.01	53.42
40.741	31.482	4.87	63.05
49.967	33.929	4.76	67.61
60.740	38.541	4.67	77.11
70.122	41.365	4.61	82.42
79.988	43.812	4.54	87.68
89.671	45.694	4.48	91.24
100.000	49.082	4.42	99.07

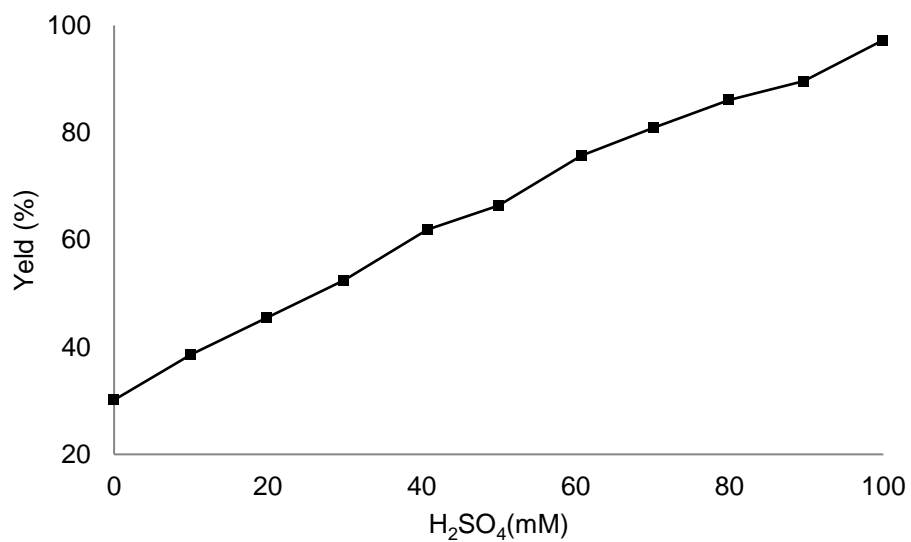


FIGURE 4.7. Yield of itaconate recovery versus sulfuric acid concentration

4.5. CONCLUSIONS

The relatively low solubility of calcium itaconate ensures that precipitation is feasible as a recovery method for IA from fermented broths. The low solubility of the salt, especially at elevated temperatures, allows the concentration of the free acid at high temperatures and precipitation as calcium salts without the need of cooling. Regeneration of the acid from the salt was possible with low concentrations of sulfuric acid. However, the formation of calcium sulfate occurs as byproduct and the fate of such a salt in industrial processes should be further evaluated. The method used to determine the solubility showed ease of application with good results. However, other methods must be evaluated in order to confirm the validity of the data obtained in this study. The spectrophotometric reading at 240nm proved to be efficient when working on pure concentrations, with its quick and easy to handle. During the itaconate recovery, it was possible to achieve a yield of 99% using 100mM concentrations of sulfuric acid.

5. SEPARATION OF ITACONIC ACID FROM AQUEOUS SOLUTION ONTO ION-EXCHANGE RESINS

This chapter has a condensed version published as a paper in 2015, with the same title: *J. Chem. Eng. Data*, **2016**, 61 (1), pp 430–437
DOI: 10.1021/acs.jced.5b00620

5.1. ABSTRACT

Itaconic acid (IA) is a promising compound that might replace part of the petrochemical-based feedstocks, such as acrylic acid, as a building block for polymers. Biotechnological developments already have allowed the production of IA by fermentation processes, but further enhancements are necessary for the recovery of the final product. This investigation examined the separation of IA from aqueous solutions using commercial strongly-basic ion-exchange resins. In order to determine the effect of the initial pH on the IA adsorption, pH values near the dissociation constants in aqueous solutions, pK_{a1} and pK_{a2} were tested (3.03, 3.85, 4.68, 5.55 and 6.33). Aiming at the analysis of the best adsorption conditions, the following temperatures were tested (10, 20, 30, 40 and 50°C). For the evaluation of equilibrium, five concentrations of IA (3.125, 6.25, 12.5, 25.0 and 50.0mM) were evaluated. The classical Freundlich and Langmuir isotherms have shown to be good fits to the experimental data, and the adsorption kinetics for IA was determined to follow a pseudo second-order (PSO) model. A new simplified mathematic model was developed and evaluated in order to determine the adsorption parameters of the fixed bed column. The experimental data of the column presented results near to the obtained from the isotherms and batch PSO. The resin PFA-300 demonstrated to be efficient for IA adsorption recovery due to its higher capacity.

5.2. INTRODUCTION

The recovery and purification of organic acids from aqueous solutions or fermentation broths is of interest in several biotechnological processes (İNCI et al., 2011). Downstream processes have significant environmental and economic impact in the process, and their improvement is essential for reduction of environmental burden and energy consumption, as well as waste production (Okabe et al., 2009). Organic acids produced *via* bioprocesses, such as citric, lactic, tartaric, gluconic and itaconic acid have long been used as intermediates in various branches of industry because they can be easily transformed into a diversity of substances (GLUSZCZ et al., 2004; WILLKE and VORLOP, 2001; SAUER et al., 2008). Therefore, the purification of these acids is extremely important and affects the quality of final products, which may be used as food additives, or pharmaceuticals and biodegradable plastic ingredients (GLUSZCZ et al., 2004).

Itaconic acid (IA) can serve as a replacement for petroleum-based compounds such as acrylic or methacrylic acids because it is equally monounsaturated (WILLKE and VORLOP 2001; KLEMENT and BÜCHS, 2013). IA is a white, crystalline, monounsaturated organic diacid with formula $C_5H_6O_4$ and a molar mass of $130.1\text{g}\cdot\text{mol}^{-1}$. It has two carboxyl groups, and a carbon-carbon double bond. Its ionization constants are $\text{pK}_{a1} \approx 3.78$ and $\text{pK}_{a2} \approx 5.38$ (ROBERTIS et al., 1990; WILLKE and VORLOP 2001). Therefore, IA is negatively charged above 4.78, and is fully ionized above pH 6.4.

Biotechnological production of IA uses *Aspergillus terreus* (WILLKE and VORLOP 2001). Its growth on renewable substrates is gaining interest for the production of this bio-based platform chemical (KLEMENT and BUCHS, 2013). Currently, IA is crystallized after filtration from the fermentation broth by cooling or by evaporation-crystallization at low pH values. However, these methods do not remove by-products synthesized during fermentation and can reduce the purity and quality of the final product (KLEMENT and BUCHS, 2013).

Synthetic ion-exchange resins have been studied in the separation and purification of organic acids (İNCI et al., 2011; LI et al., 2010; NAM et al., 2011; GLUSZCZ et al., 2004; JUN et al., 2007). These resins can adsorb molecules selectively, while the other components of the solution flow through the adsorbent.

The adsorbed product can be recovered subsequently by eluting the loaded. Despite the existing knowledge of the principles of separation of organic acids by ion-exchange methods, there are details that must be further developed for specific systems, such as the effective solute load, or the kinetics of adsorption. Therefore, the objective of this study was to evaluate the separation of IA from aqueous solutions by using two cationic ion-exchange synthetic resins.

5.3. MATERIAL AND METHODS

5.3.1. Determination Batch Adsorption Parameters

The tests were performed in 250ml Erlenmeyer flasks containing 100ml of IA solution and 2.00g of adsorbent. All assays were made in an orbital shaker at 28°C with agitation at 120rpm. The resins were activated after serial washing with hydrochloric acid (2N), deionized water, sodium hydroxide (2N) and further washing with deionized water. The initial Itaconic Acid (denoted IA, Aldrich Company Co., ≥99%) solutions were prepared with concentrations of 50mM and initial pH was adjusted to 3.85. Previous analysis showed that the tested resins reached adsorption equilibrium in about 30 minutes, as the tests were performed considering 1h of reaction. The experiments were conducted following the steps of the schematic diagram of FIGURE 5.1.

The experiments covered two types of strongly basic resins available on the market: *Purolite A-500P* and *PFA-300*. The main physical and chemical characteristics of the resins are described in TABLE 5.1. In order to determine the effect of the initial pH on IA adsorption, pH values near the dissociation constants in aqueous solutions, pK_{a1} (3.66-3.89) and pK_{a2} (5.21-5.55) (ROBERTIS et al., 1990; WILLKE AND VORLOP 2001), were tested. IA solutions at different pH, of 3.03, 3.85, 4.68, 5.55 and 6.33 were prepared. The pH was adjusted with HCl 0.1N.

Aiming at the analysis of the best adsorption conditions, the following temperatures were tested: 10, 20, 30, 40 and 50°C. The IA solution was prepared with an initial pH of 3.85.

TABLE 5.1. Typical physical and chemical characteristics of the resins

Parameters	<i>Purolite A-500P</i>	<i>Purolite PFA-300</i>
Polymer matrix structure	Macroporous styrene-divinylbenzene	Crosslinked gel polystyrene
Physical form and appearance	Opaque near-white spheres	Amber spherical beads
Functional groups	R-(CH ₃) ₃ N ⁺	R-(CH ₃) ₂ (C ₂ H ₄ OH)N ⁺
Shipping weight (g/l)	655 – 685	690
Particle size range (mm)	0.850 – 0.600	0.710 – 0.425
Moisture retention (%)	63 – 70	40 – 45
Total exchange capacity (eq/l.min)	0.8	1.4

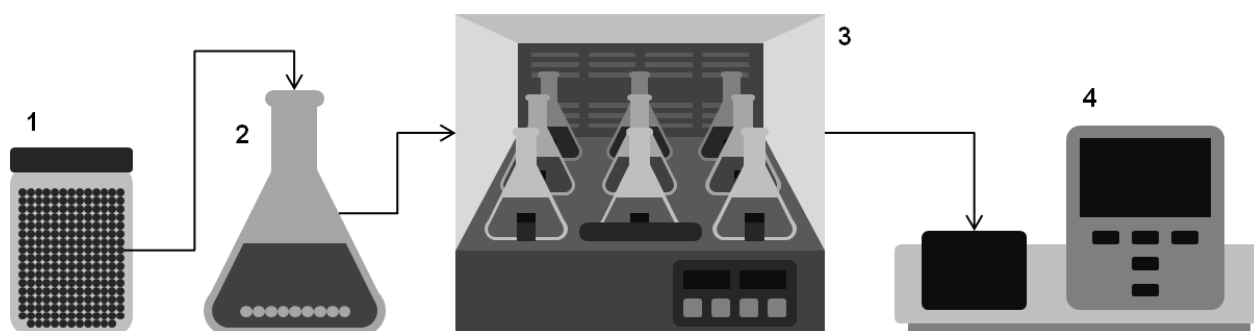


FIGURE 5.1. Determination batch adsorption parameters
(1) ion-exchange resin, (2) IA solution, (3) Shaker incubator and (4) Spectrophotometer

5.3.2. Determination of Adsorption Isotherms

For the modeling of adsorption isotherms, the models of Freundlich and Langmuir were evaluated. Solutions with five different concentrations for IA: 3.125, 6.25, 12.5, 25.0 and 50.0mM were prepared, and equilibrated with the resins. The relation between the solid-phase concentrations (q) at equilibrium was calculated through a material balance:

$$q = \frac{(C_0 - C)\rho V}{m} \quad (1)$$

where C_0 and C are, respectively, the initial concentration and the equilibrium concentration of IA in the liquid-phase (mM), ρ is the molecular weight ($\text{g}\cdot\text{mol}^{-1}$), V is the solution volume (l) and m is the mass of wet resin (g).

The Langmuir isotherm is one of the standard models to calculate the adsorption equilibrium parameters, which is defined based on the assumption that distribution of pores in the surface of the adsorbent is homogeneous, with negligible interaction forces between adsorbed molecules. The equation for a fixed temperature is given below (LANGMUIR, 1915; SEADER et al., 2010):

$$q = \frac{q_s \cdot K_L \cdot C}{1 + K_L \cdot C} \quad (2)$$

where q_s is the saturation capacity of the resin, i.e., the maximum solid-phase concentration of IA in equilibrium, and K_L is the Langmuir equilibrium constant, related to the adsorption site affinity (SEADER et al., 2010).

The values of q_s and K_L were determined by linear regression using equation (3), a linearized form of equation (2): in this case, the slope is $(1/q_s)$ and the intercept is $(1/(K_L \cdot q_s))$, the values of q_s and K_L may be calculated from the linear regression coefficients.

$$\frac{C}{q} = \frac{1}{q_s \cdot K_L} + \frac{1}{q_s} C \quad (3)$$

The other isotherm used, also classical, was the Freundlich model, equation (4). (FREUNDLICH, 1910; SEADER et al., 2010):

$$q = K_F \cdot C^{1/n} \quad (4)$$

where K_F and n are temperature-dependent constants for a specific solute and adsorbent.

Equation (4) is exponential, and its linearized form is the logarithm of both sides of the equation (5):

$$\ln q = \ln K_F + \left(\frac{1}{n}\right) \cdot \ln C \quad (5)$$

Using the linear regression of (5), the is intercept $\ln K_F$ and the slope is $(1/n)$, so that values of K_F and n may be calculated.

The investigation of the adsorption kinetics was done by collecting 0.5ml samples every 3min for 1h of equilibration time. These experimental data were analyzed using a pseudo second-order (PSO) model. Ho and Mckay deduced the simple linear equation of a PSO for the analysis of adsorption kinetics from liquid solutions (HO and MCKAY, 1998; HO and MCKAY, 1999a; HO and MCKAY, 1999b):

$$\frac{dq}{dt} = k_2 \cdot (q_e - q)^2 \quad (6)$$

where q_e is the amount of solute adsorbed at equilibrium ($\text{g}\cdot\text{g}^{-1}$) and k_2 is the PSO rate constant of sorption ($\text{g}\cdot\text{g}^{-1}\cdot\text{min}^{-1}$) (WU et al., 2009). Integrating equation (6), for the initial conditions $Q(0) = 0$, and rearranging to obtain a linear form:

$$\frac{t}{q} = \left(\frac{1}{k_2 \cdot q_e^2} \right) + \left(\frac{1}{q_e} \right) \cdot t \quad (7)$$

A linear regression of t/q as a function of t will give, comparing with equation (7), a slope of $1/q_e$ and an intercept $1/(k_2 \cdot q_e^2)$, from which the values of q_e and k_2 may be isolated.

The error was calculated using the linear regression coefficient (R^2), equation (8), to compare the model and the experimental results:

$$R^2 = 1 - \frac{SSR}{SST} \quad (8)$$

$$SSR = \sum_{i=1}^n (y_{exp} - y_{calc})_i^2 \quad (9)$$

$$SST = \sum_{i=1}^n (y_{exp})_i^2 - \frac{1}{n} \left(\sum_{i=1}^n y_{exp} \right)^2 \quad (10)$$

where SSR and SST are the residual and total sum of squares, respectively, n is the number of data points, y_{calc} is the calculated value, and y_{exp} is the measured value of the experiment.

The concentration of IA in equilibrium solutions was analyzed by reading the absorbance at a wavelength of 240nm, with an extinction coefficient of $3.14\text{mM}^{-1}\cdot\text{cm}^{-1}$. Samples of 0.5ml each were collected and diluted to 4.5ml of phosphate buffer solution at pH 7.0.

5.3.3. Determination of the Fixed-Bed Continuous Adsorption Parameters

The experiments in fixed bed column were performed to remove IA from aqueous solution with a concentration of 400mM and an initial pH 3.85. The schematic diagram of the experimental setup is shown in FIGURE 5.2. Two glass columns with an internal diameter of 1.0cm were used as fixed bed column. The adsorbent bed was packed with *Purolite PFA-300* and *A-500P* resins using stepwise procedure. Initially, 10.0g of the adsorbent were manually poured into each column until all material got packaged. Then the column was washed and activated with a sequence of 500ml of deionized water, 200ml of HCl (2N), 500ml of deionized water and 200ml of NaOH (2N). Samples were taken every 2 minutes under a flow of $0.825\pm 0.034\text{ml}\cdot\text{min}^{-1}$.

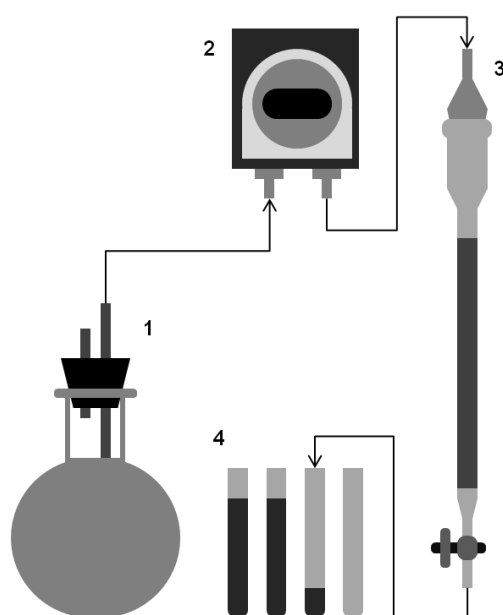


FIGURE 5.2. Experimental fixed-bed continuous adsorption (1) feed of IA solution; (2) peristaltic pump; (3) fixed-bed column; (4) outlet collection

5.3.4. Mathematical modeling of the fixed bed adsorption column

A mathematical model for adsorption in fixed bed ion exchange column was developed and verified experimentally. The model approaches four transfer stages: mass transfer in the bulk liquid, diffusion in the liquid film, intraparticle transfer, and adsorption equilibrium reaction (XU et al., 2013). Thus, each mass transfer step will be developed separately in a first approach. These steps will be later combined in the transition boundary of each region: bulk liquid, liquid film and adsorbent particle (FIGURE 5.3).



FIGURE 5.3. Scheme of the main stages and directions in the mass transfer of the fixed bed adsorption column: (white area) bulk liquid; (gray area) liquid film; (black area) adsorbent particle

The mass transfer in the bulk liquid basically describes the complete filling of the adsorbate along the entire fixed bed column (FIGURE 5.4). During the course, while the accumulation occurs on the porosity of the bed and of the resin, both convective motions and dispersions (axial and radial) also occur.

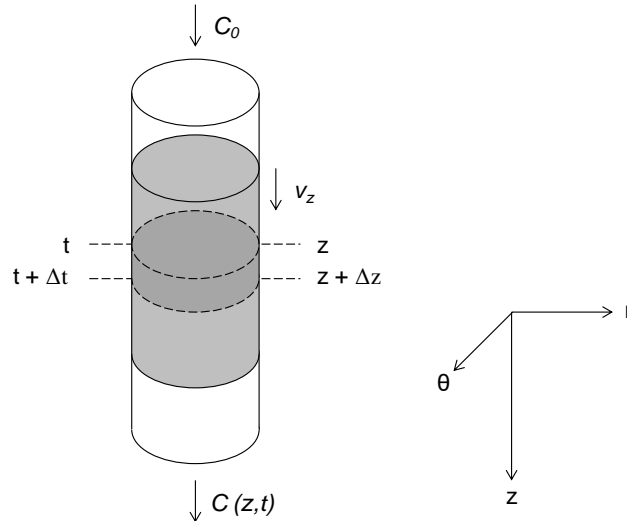


FIGURE 5.4. Mass transfer in accordance with the movement through the adsorption bed

Assuming that all cross sections are homogeneous and the radial movement can be neglected, the mass balance for the solute in the bulk phase flows along the bed height as follows:

$$\text{Input} - \text{Output} + \text{Generation} - \text{Consumption} = \text{Accumulation} \quad (11)$$

The following assumptions were made to formulate the model equations:

1. Chemical reactions do not occur in the column;
2. Adsorption is an isothermal and isobaric process;
3. The particles that make up a solid phase of fixed bed are spherical, uniform in size and homogeneous;
4. The dispersion in the radial direction of the bed is negligible;
5. The diffusion is based in the second Fick's law;
6. The flow rate is constant and invariant with the column position;

Thus, the mass conservation equation for the solute in the bulk liquid that flows over the bed is acquired to represent the relationship between corresponding changes in the equations (12):

$$A \cdot [N_{IA}|_z - N_{IA}|_{z+\Delta z}] = A \cdot \Delta z \cdot \frac{\partial C_{IA}}{\partial t} \quad (12)$$

where A is the flow area, N_{IA} is the mass flow of IA, z is distance to the inlet, C_{IA} is the concentration of the IA in the bed and t is time.

Equation (12) can be rearranged as follows (BIRD et al., 2006; SEADER, 2010):

$$-\frac{\partial N_{IA}}{\partial z} = \frac{\partial C_{IA}}{\partial t} \quad (13)$$

The mass flow can be divided in two steps, diffusion and movement:

$$N_A = J_{IAz} + C_{IA} \cdot v_z \quad (14)$$

where J_{IAz} is the diffusivity ($-D \cdot \nabla C_{IA}$), D_z is the diffusivity bed constant and ∇C_{IA} is the concentration by cylindrical coordinates ($\frac{\partial C_{IA}}{\partial r} + \frac{1}{r} \frac{\partial C_{IA}}{\partial \theta} + \frac{\partial C_{IA}}{\partial z}$) and v_z is the linear bed velocity (BIRD et al., 2006; SEADER, 2010).

Combining the equation (13) and (14), with negligible radial diffusivity, leads to the final relation:

$$\frac{\partial C_{IA}}{\partial t} = D_z \cdot \frac{\partial^2 C_{IA}}{\partial z^2} - v_z \frac{\partial C_{IA}}{\partial z} \quad (15)$$

This simplified mathematical model describes the concentration of IA along the column length, z axis, according to the change in time. The bed accumulation is divided into two phases: solid and liquid, those are related to the porosity factor or void fraction:

$$\varepsilon = \frac{V_l}{V_t} = 1 - \frac{V_s}{V_t} \quad (16)$$

$$C_{IA} = \varepsilon \cdot C + (1 + \varepsilon) \cdot q \quad (17)$$

where C is the acid concentration in the liquid phase, q is the acid concentration in the solid phase, ε is the ion exchange bed porosity, V_t , V_l and V_s are bed, bulk and adsorbent volume, respectively.

Gathering the equations (15) and (17) and negligible diffusion and dispersion effects in the adsorbent, we arrive at:

$$\varepsilon \cdot \frac{\partial C}{\partial t} + (1 - \varepsilon) \cdot \frac{\partial q}{\partial t} = \varepsilon \cdot D_l \cdot \frac{\partial^2 C}{\partial z^2} - \varepsilon \cdot v_l \frac{\partial C}{\partial z} \quad (18)$$

where D_l is the diffusivity bulk constant (D_z/ε) and v_l is the linear liquid velocity (v_z/ε).

The initial and boundary conditions are:

$$t = 0 \begin{cases} C(z, 0) = 0 \\ q(z, 0) = 0 \end{cases} \quad (19)$$

$$z = 0 \begin{cases} t = 0 \rightarrow C(0, 0) = 0 \\ t > 0 \rightarrow C(0, t) = C_0 \end{cases} \quad (20)$$

$$z = H \rightarrow \frac{\partial C}{\partial z} = 0 \quad (21)$$

The partial differential equations (15) to (21) are solved numerically by reducing a set of nonlinear algebraic equations using explicit finite difference technique. A mathematical algorithm to solve these equations is developed and implemented in a computer program using MATLAB software (2014.b). The error was calculated using the SSR, equation (9).

5.4. RESULTS AND DISCUSSION

5.4.1. Effect of pH in the Adsorption

The pH and temperature of the system may affect both the adsorbent and the solute. In the case of strong anion exchangers, the influence of pH is apparent only at extreme pHs. But for ionizable solutes such as IA, pH affects the species

distribution, and that may affect the adsorption. Temperature has a more complex effect, because it alters both equilibrium and kinetics, although the range of temperature recommended for the resins is narrowing (typically ambient). Adsorption of IA from aqueous solutions was evaluated at five different initial pHs with a 50mM concentration, using two ion-exchange resins, in order to analyze the effect of initial pH on adsorption. It was observed (TABLE 5.2) that when the initial pH is near the value of the first IA dissociation constant, pK_{a1} , i.e. when only one carboxyl groups of the IA molecule is deprotonated, *A-500P* resin has a higher adsorption capacity. In the case of *PFA-300* resin, the adsorption capacity is inversely proportional to initial pH. When the initial pH exceeds pK_{a2} , the ability of the resin to adsorb IA decreases and tends to equilibrium as shown in FIGURE 5.5. This may be due to deprotonation of the two carboxylic groups of the acid, when the same IA molecule competes to bind more than one of the active sites of the resin.

TABLE 5.2. Effect of initial pH on the adsorption of IA onto ion-exchange resins

pH	T (°C)	m_{resin} (g)	C_0 (g.l ⁻¹)	C_e (g.l ⁻¹)	q (g.g ⁻¹)
<i>A-500P</i>					
3.03	28	2.00	6.505	4.717±0.087	0.089±0.004
3.85	28	2.00	6.505	4.449±0.159	0.103±0.008
4.68	28	2.00	6.505	4.717±0.031	0.089±0.002
5.50	28	2.00	6.505	4.960±0.060	0.077±0.003
6.33	28	2.00	6.505	5.064±0.157	0.072±0.008
<i>PFA-300</i>					
3.03	28	2.00	6.505	3.282±0.096	0.161±0.005
3.85	28	2.00	6.505	3.532±0.027	0.149±0.001
4.68	28	2.00	6.505	4.010±0.015	0.125±0.001
5.50	28	2.00	6.505	4.495±0.029	0.101±0.001
6.33	28	2.00	6.505	4.571±0.088	0.097±0.004

(pH) Initial pH of IA solution; (T) adsorption temperature; (m_{resin}) adsorbent mass; (C_0) initial concentration of IA solution; (C_e) equilibrium concentration; (q) adsorbed adsorbate

The results achieved by the one-way analysis of variance (ANOVA) showed that the initial pH in IA solution has a significant impact for adsorption in both resins. The F-test presented for *A-500P* and *PFA-300*, respectively, a value of 13.89 and 260.39 to F-critical of 3.48 with 4 degrees of freedom. As F-test is greater than F-critical, this hypothesis can be confirmed at the risk of 5%. These experimental data

are in accordance with Gulicovski et al. (2008), who concluded that the IA adsorption onto alumina surface is extremely pH dependent and the maximum adsorption occurs at a pH near the value of pK_{a1} .

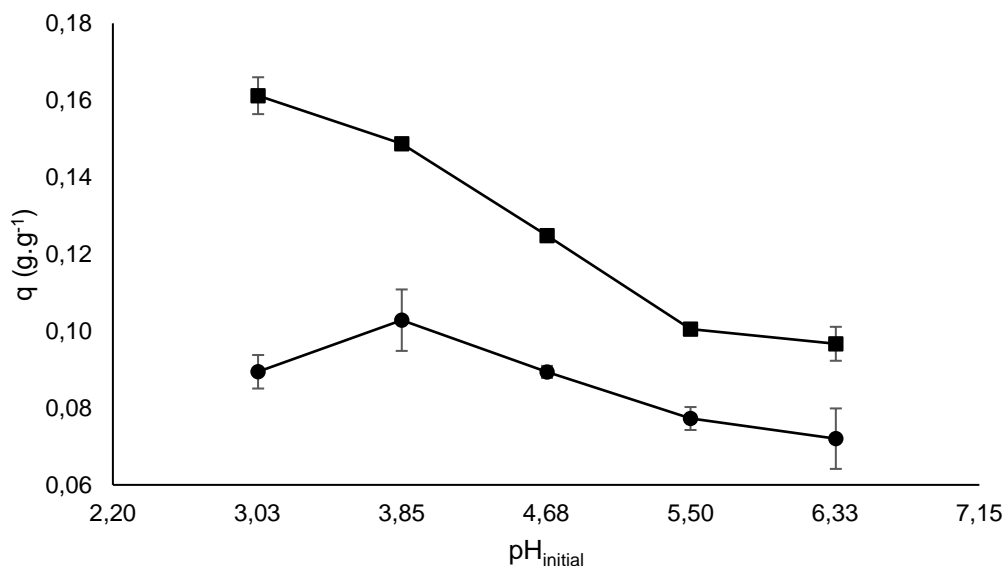


FIGURE 5.5. Effect of initial pH on the adsorption of IA onto ion-exchange resins (●) *A-500P*; (■) *PFA-300*

5.4.2. Effect of Temperature in the Adsorption

The results of IA adsorption on the resins at different temperatures, ranging from 10 to 50°C, are showed in the TABLE 5.3 and FIGURE 5.6. The results of an ANOVA show that the temperature of adsorption do not have a significant impact in the adsorption using *PFA-300* resin in the tested conditions. The F-test presenting a value of 2.57 to an F-critical of 3.48 with 4 degrees of freedom. In the case of the *A-500P* resin, it presented an F value of 3.74 over the temperature range 10-50°C, but this value decreased to 2.94 at temperatures lower than 40°C.

TABLE 5.3. Effect of temperature on the adsorption of IA onto ion-exchange resins

pH	T ($^{\circ}C$)	m_{resin} (g)	C_0 (g.l $^{-1}$)	C_e (g.l $^{-1}$)	q (g.g $^{-1}$)
<i>A-500P</i>					
3.85	10	2.00	6.505	4.515±0.023	0.099±0.001
3.85	20	2.00	6.505	4.549±0.035	0.098±0.001
3.85	30	2.00	6.505	4.558±0.031	0.097±0.001
3.85	40	2.00	6.505	4.584±0.025	0.096±0.001
3.85	50	2.00	6.505	4.668±0.099	0.092±0.004
<i>PFA-300</i>					
3.85	10	2.00	6.505	3.547±0.038	0.148±0.002
3.85	20	2.00	6.505	3.498±0.064	0.150±0.003
3.85	30	2.00	6.505	3.588±0.086	0.146±0.004
3.85	40	2.00	6.505	3.618±0.086	0.144±0.004
3.85	50	2.00	6.505	3.657±0.044	0.142±0.002

(pH) Initial pH of IA solution; (T) adsorption temperature; (m_{resin}) adsorbent mass; (C_0) initial concentration of IA solution; (C_e) equilibrium concentration; (q) adsorbed adsorbate

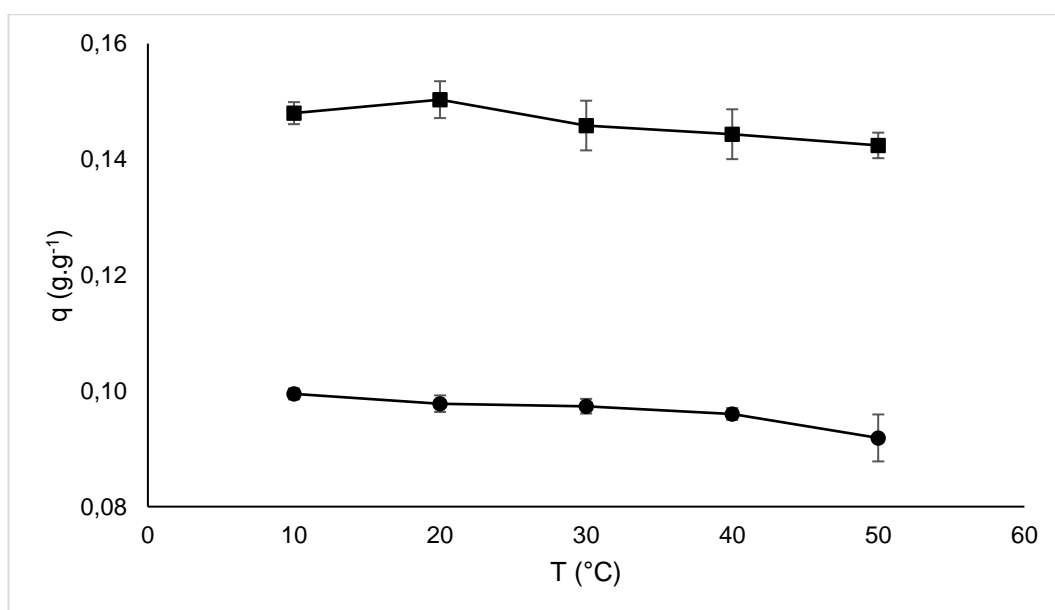


FIGURE 5.6. Effect of temperature on the adsorption of IA onto ion-exchange resins (●) A-500P; (■) PFA-300

5.4.3. Effect of Initial Acid Concentration in the Adsorption

The effect of initial acid concentration on adsorption onto resins was evaluated at five different initial IA concentrations from 3.125 to 50mM. It was observed (TABLE 5.4) that when the initial acid concentration raised the equilibrium concentration increased by an ever smaller extent. This was expected, and is due to the saturation

of the ion-exchange sites of the resins, preventing that more binding between free acid and the adsorbent occurs. FIGURE 5.7 shows that the equilibrium concentrations increased from 0.02g.g^{-1} to 0.10g.g^{-1} for *A-500P* and to 0.15g.g^{-1} for *PFA-300*.

TABLE 5.4. Effect of initial concentration of acid on the adsorption of IA onto ion-exchange resins

pH	T ($^{\circ}\text{C}$)	m_{resin} (g)	C_0 (g.l^{-1})	C_e (g.l^{-1})	q (g.g^{-1})
<i>A-500P</i>					
3.85	28	2.00	0.407	0.012 ± 0.007	0.020 ± 0.000
3.85	28	2.00	0.813	0.054 ± 0.004	0.038 ± 0.000
3.85	28	2.00	1.626	0.526 ± 0.008	0.055 ± 0.000
3.85	28	2.00	3.253	1.791 ± 0.008	0.073 ± 0.000
3.85	28	2.00	6.505	4.600 ± 0.032	0.095 ± 0.002
<i>PFA-300</i>					
3.85	28	2.00	0.407	0.021 ± 0.010	0.019 ± 0.000
3.85	28	2.00	0.813	0.021 ± 0.011	0.040 ± 0.001
3.85	28	2.00	1.626	0.099 ± 0.004	0.076 ± 0.000
3.85	28	2.00	3.253	0.959 ± 0.016	0.115 ± 0.001
3.85	28	2.00	6.505	3.517 ± 0.032	0.149 ± 0.002

(pH) Initial pH of IA solution; (T) adsorption temperature; (m_{resin}) adsorbent mass; (C_0) initial concentration of IA solution; (C_e) equilibrium concentration; (q) adsorbed adsorbate

5.4.4. Langmuir Isotherm

The results demonstrate that the Langmuir isotherm explains the experimental data especially at low concentrations of IA, with a maximum capacity of 0.095g.g^{-1} for the resin *A-500P* and 0.149g.g^{-1} for the resin *PFA-300*, respectively. The values of K_L and q_0 , the parameters calculated using the Langmuir equation, are presented in TABLE 5.5, and a graphic representation of the curves is presented in FIGURE 5.7. One may notice that the curve generated by the Langmuir isotherm presents deviations mainly before saturation of the resins. However, the values of the q_0 represent realistic, saturation capacity of both resins.

TABLE 5.5. Langmuir isotherm parameters for the adsorption of IA onto ion-exchange resins

Resin	q_S	K_L	R^2
<i>A-500P</i>	0.097	0.244	0.985
<i>PFA-300</i>	0.154	0.147	0.995

(q_S) Saturation capacity of the resin; (K_L) the Langmuir equilibrium constant

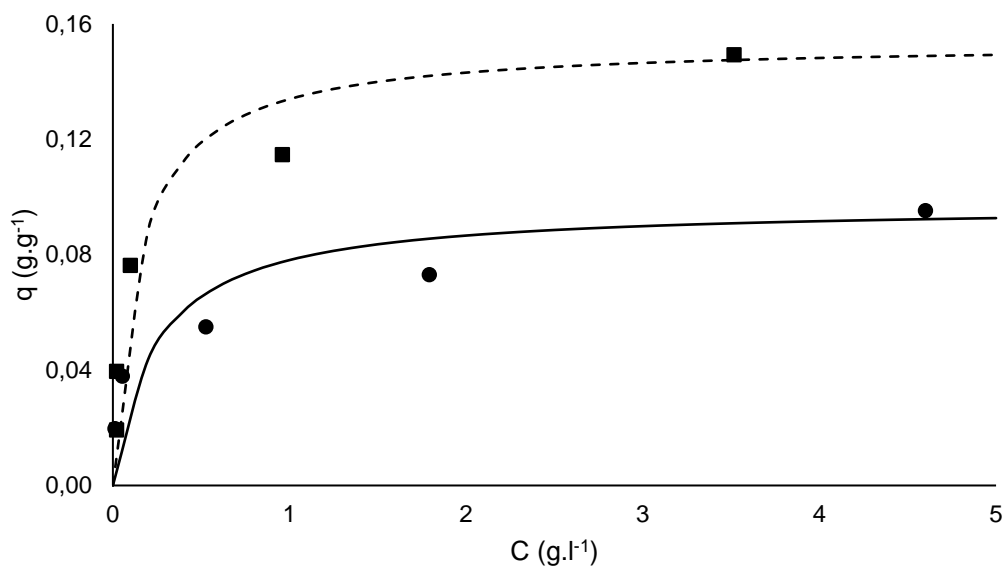


FIGURE 5.7. Langmuir isotherm for the adsorption of IA onto ion-exchange resins
 (●) *A-500P*; (■) *PFA-300*; (—) Langmuir isotherm of *A-500P*; (- - -) Langmuir isotherm of *PFA-300*

5.4.5. Freundlich Isotherm

Unlike the Langmuir Isotherm, the curve generated by the Freundlich equation did not coincide with the experimental values of the *PFA-300* resin. However, this model proved to be good for the adsorption of the resin *A-500P*. FIGURE 5.8 shows the plot of the Freundlich equation isotherm for IA adsorption for both adsorbents. Results for adjustment of the Freundlich equation to the experimental data are presented in TABLE 5.6.

TABLE 5.6. Freundlich isotherm parameters for the adsorption of IA by ion-exchange resins

Resin	K_F	n	R^2
<i>A-500P</i>	0.0656	4.0502	0.970
<i>PFA-300</i>	0.1128	3.0239	0.836

(K_F) temperature-dependent constant for a specific solute; (n) temperature-dependent constants for a specific adsorbent

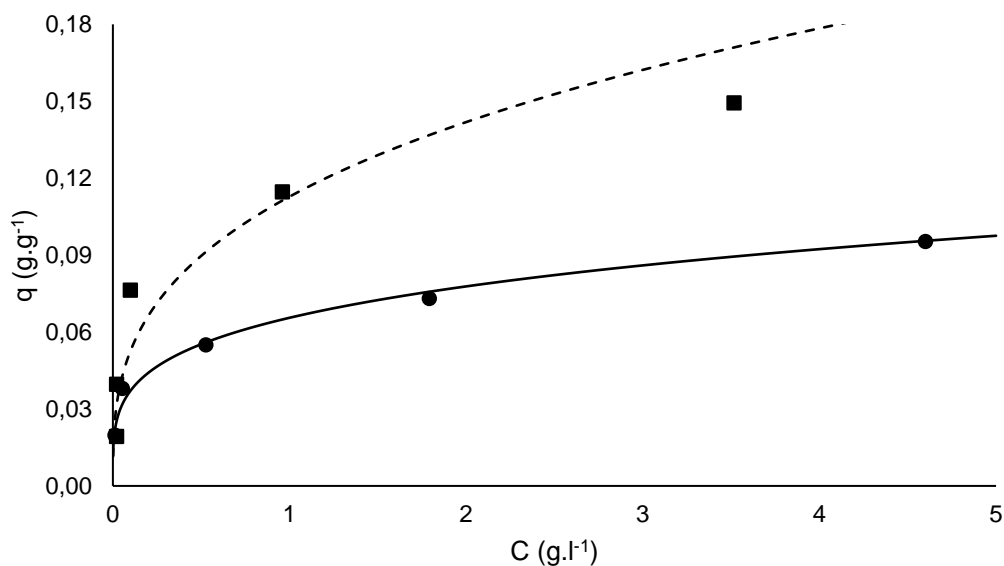


FIGURE 5.8. Freundlich isotherm for the adsorption of IA onto ion-exchange resins (●) *A-500P*; (■) *PFA-300*; (—) Freundlich isotherm of *A-500P*; (- - -) Freundlich isotherm of *PFA-300*

5.4.6. Effect of Contact Time on the Adsorption

TABLE 5.7 shows the effect of contact time on the adsorption of IA for each resin, studied over a period of 1.0 h. The adsorption demonstrated to be faster in the early stages when the acid contacts the adsorbent, and subsequently becomes slower when the resin reaches equilibrium. This is expected because of a large number of sites is available for adsorption in the surface of the resin at the beginning of the process, and the higher solute concentration in aqueous phase favors the association (RAJORIYA et al., 2007; INCI, 2011).

TABLE 5.7. Effect of contact time of IA on the adsorption

t (min)	<i>A-500P</i>		<i>PFA-300</i>	
	C (g.l ⁻¹)	q (g.g ⁻¹)	C (g.l ⁻¹)	q (g.g ⁻¹)
0	6.505	0.000	6.505	0.000
3	5.385±0.112	0.056±0.006	5.179±0.019	0.066±0.001
6	5.045±0.027	0.073±0.001	4.694±0.123	0.090±0.006
9	4.768±0.099	0.086±0.005	4.415±0.059	0.103±0.003
12	4.681±0.029	0.090±0.001	4.248±0.016	0.111±0.001
15	4.617±0.013	0.093±0.001	4.118±0.035	0.117±0.002
18	4.584±0.053	0.094±0.003	4.031±0.056	0.121±0.003
21	4.564±0.045	0.094±0.002	3.926±0.029	0.125±0.001
24	4.522±0.008	0.096±0.000	3.807±0.032	0.130±0.002
27	4.562±0.048	0.093±0.002	3.799±0.000	0.130±0.000
30	4.530±0.067	0.094±0.003	3.773±0.027	0.130±0.001
33	4.520±0.016	0.094±0.001	3.795±0.091	0.129±0.004
36	4.567±0.083	0.092±0.004	3.686±0.016	0.133±0.001
39	4.549±0.013	0.092±0.001	3.692±0.040	0.132±0.002
42	4.466±0.013	0.095±0.001	3.686±0.016	0.132±0.001
45	4.577±0.112	0.090±0.005	3.701±0.059	0.130±0.003
48	4.515±0.008	0.092±0.000	3.671±0.005	0.131±0.000
51	4.509±0.101	0.092±0.005	3.661±0.019	0.131±0.001
54	4.486±0.048	0.092±0.002	3.661±0.003	0.130±0.000
57	4.460±0.048	0.093±0.002	3.642±0.008	0.130±0.000
60	4.517±0.005	0.090±0.000	3.618±0.048	0.131±0.002

(C) equilibrium concentration; (q) adsorbed adsorbate

5.4.7. Pseudo-Second Order Equation

The values of q_e and k_2 shown in TABLE 5.8, were obtained from the slopes and intercepts of linearized data from TABLE 5.7 using the standard pseudo-second order model. As it can be observed in FIGURE 5.9, this model was suitable for adsorption kinetics, especially after saturation of both resins. However, during the initial adsorption of *A-500P* resin, there was a greater deviation from the mathematical model and experimental data. Such disparity did not occur for the *PFA-300* resin.

TABLE 5.8. Pseudo-Second Order Equation parameters for the adsorption kinetics of IA onto ion-exchange resins

Resin	q_e	k_2	R^2
<i>A-500P</i>	0.093	22.970	0.998
<i>PFA-300</i>	0.138	2.971	0.999

(q_e) amount of solute adsorbed at equilibrium; (k_2) PSO rate constant of sorption

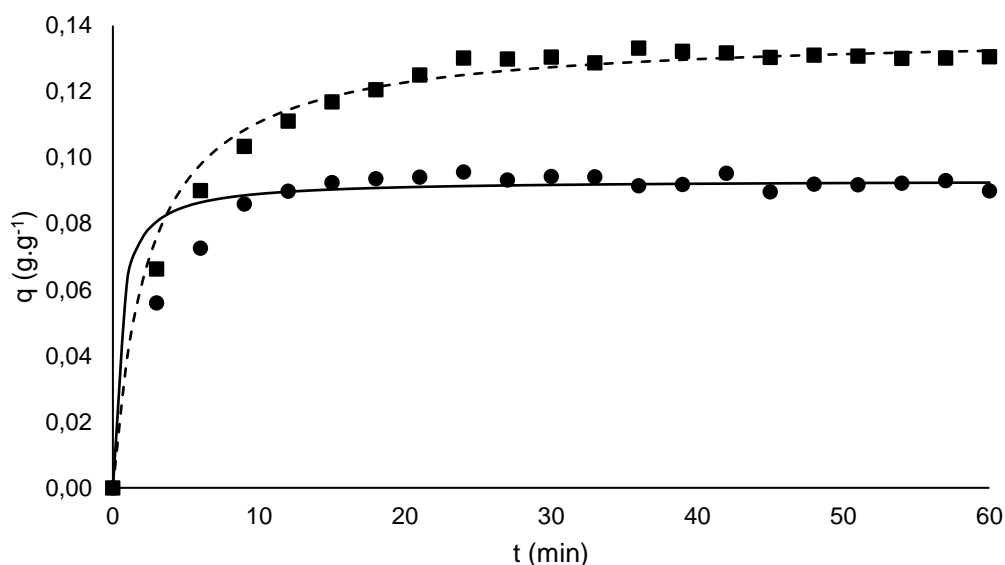


FIGURE 5.9. Pseudo-Second Order equation for the adsorption kinetics of IA onto ion-exchange resins

(●) *A-500P*; (■) *PFA-300*; (—) PSO equation *A-500P*; (- - -) PSO equation isotherm *PFA-300*

5.4.8. Fixed-Bed Continuous Adsorption Parameters

Previous experiments determined the optimal control conditions for IA adsorption. In this section, the fixed bed column was made in order to compare two resins: *PFA-300* and *A-500P*. Equal amounts of 10.0g each of both resins dried in an IA flux of $0.825 \pm 0.034 \text{ ml} \cdot \text{min}^{-1}$ were used in the elution and adsorption tests. The math was adjusted taking into account the effect of humidity, washing and activation of the resins. Secondary experiments determined that the relation between the masses of activated and dried resin were 1.637 ± 0.006 and $1.499 \pm 0.006 \text{ g} \cdot \text{g}^{-1}$ respectively, for *A-500P* and *PFA-300*. The resin *A-500P* reached saturation faster

than the resin *PFA-300*, as shows in FIGURE 5.10. The *A-500P* took approximately 30min to reach adsorbate saturation, while the *PFA-300* took 50min.

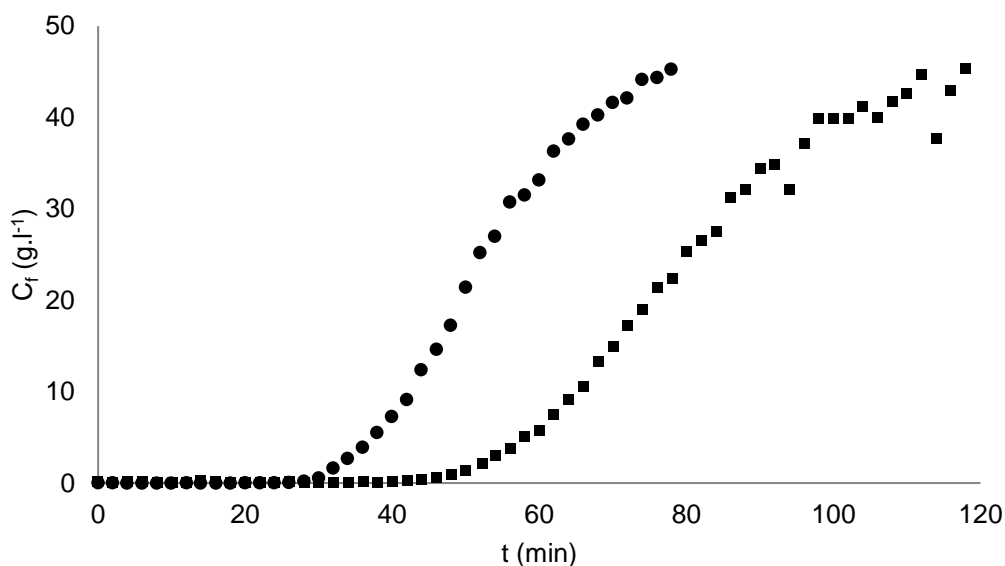


FIGURE 5.10. IA concentration in the fixed bed column outlet (C_f)
(●) *A-500P*; (■) *PFA-300*)

The analysis of the adsorption effects can be evaluated through the graphic in FIGURE 5.11, which represents the resin saturation through the IA concentration in the exit of the fixed bed column. As previously seen, the saturation capacity was determined by the Langmuir isotherm and by PSO kinetics, resulting in 0.097 and 0.093g.g⁻¹ for *A-500P* and 0.154 and 0.138g.g⁻¹ for *PFA-300*, respectively. The adsorption column presented experimental values near to the calculated: 0.083 and 0.135g.g⁻¹ for *A-500P* and *PFA-300*, respectively. However, the fixed bed presents diffusion and dispersion effects, which do not occur in the batch process. Besides, there is also accumulation in the bulk liquid, considerably rising IA accumulation in the column.

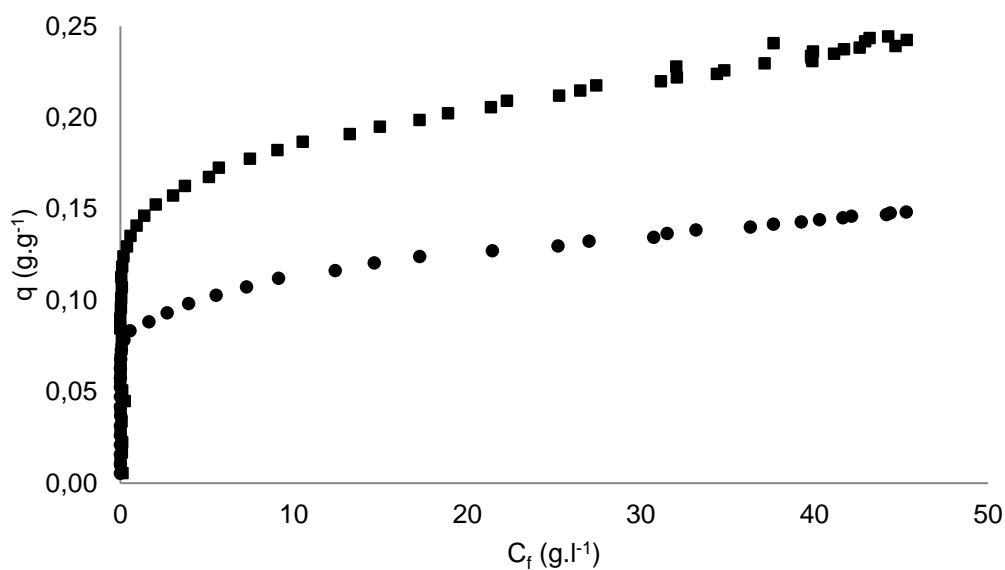


FIGURE 5.11. Relation between adsorption and IA concentration in the fixed bed column outlet (●) A-500P; (■) PFA-300)

The elution tests were made to evaluate the IA release potential of the resins. Using HCl with the same molar concentration as IA in the adsorption experiment (400mM), it was possible to determine a concentration curve, FIGURE 5.12. By presenting less amounts of adsorbed IA, the resin A-500P was washed faster than the resin PFA-300. Both resins began to elute in approximately 20min, minimal necessary time for the solution to flow through the whole extension of the column. The A-500P washing was completed after approximately 40min, half the time necessary to the elution of PFA-300.

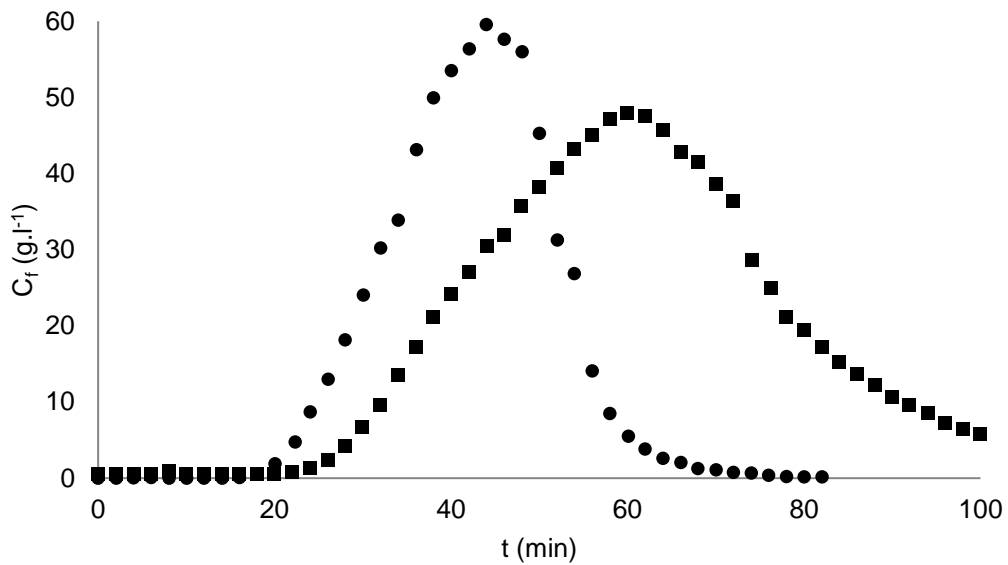


FIGURE 5.12. IA elution from ion-exchange resins in fixed bed column.
(●) *A-500P*; (■) *PFA-300*)

5.4.9. Determination of the Mathematical Model of the Fixed Bed Adsorption Column

A simplified model of the mass balance was used to determine the operational parameters involved in fixed bed column adsorption, equation (9). Thus, the diffusivity constant and dispersion velocity lengthwise the fixed bed column were determined and presented in TABLE 5.9. The simplified model was adjusted with the experimental data reaching R^2 of 0.937 and 0.994 for *A-500P* and *PFA-300*, respectively (FIGURE 5.13).

The dispersion velocity (v_l) to the bulk liquid was determined through direct calculation of the volumetric flux and the cross section area ($v_l = f/A$). The volumetric flux was measured averaging all the samples and the area was determined by the calculation of the circle with a radius of 0.05dm. The relation between v_z e v_l was used to determine the porosity ($v_z = \varepsilon \cdot v_l$). Thus, the coefficient of diffusivity of the bulk liquid was determined using that porosity.

TABLE 5.9. Calculated values of the experimental fixed bed column model parameters

Parameters	PFA-300	A-500P
D_z (dm ³ .s ⁻¹)	1.59E-05	1.77E-05
v_z (dm.s ⁻¹)	3.63E-04	5.83E-04
f (dm ³ .s ⁻¹)	1.37E-05	1.38E-05
A (dm ²)	7.85E-03	7.85E-03
D_l (dm ³ .s ⁻¹)	7.60E-05	5.35E-05
v_l (dm.s ⁻¹)	1.74E-03	1.76E-03
ε	0.209	0.331

D_z is the diffusivity bed constant, v_z is the linear bed velocity, f is the volumetric flow, A is the flow area, D_l is the diffusivity bulk constant, v_l is the linear liquid velocity and ε is the ion exchange bed porosity

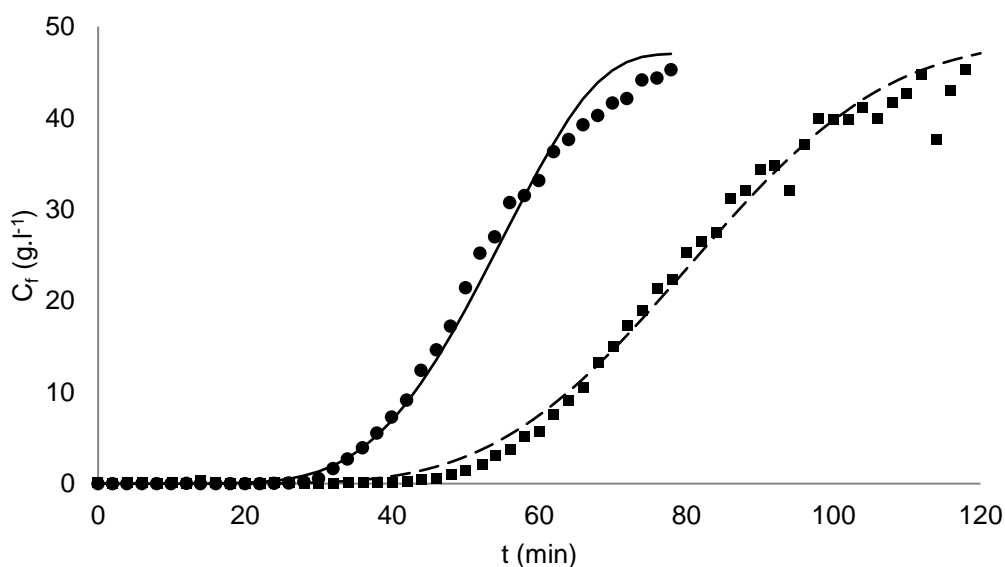


FIGURE 5.13. Mathematical model of the fixed bed column
 (●) A-500P; (■) PFA-300; (—) Mathematical model of A-500P; (- - -) Mathematical model of PFA-300

5.5. CONCLUSIONS

This experiment aimed to define the adsorption parameters of itaconic acid (IA) in commercial ion-exchange resins. The following parameters were investigated: the effect of contact time, the initial concentration and the initial pH of the IA solution, and the temperature during adsorption of resins *Purolite PFA-300* and *A-500P*. It was observed that the IA recovery decreases with increasing concentration of acid. It was found that the *PFA-300* resin has greater capacity to recover IA at lower pH and the

resin *A-500P* showed higher adsorption when pH is near pK_{a1} (3.85). The results showed that the IA adsorption resin can be well described with both the Freundlich and Langmuir isotherms. The experimental equilibrium data were well explained by the equations, and adequate conditions for IA adsorption in ion-exchange resins could be defined. The results showed that the *PFA-300* resin is a more effective adsorbent for IA removal from aqueous solutions. However, the *A-500P* resin presents a faster saturation rate compared with *PFA-300*. Studies about adsorption in fixed bed column confirmed the batch analysis, and the experimental data are closer to the Langmuir isotherm. The simplified mathematic model, or fixed bed mass balance, proved to be efficient in determining the control parameters. Further studies about the intraparticle and intrafilm effects are necessary to prove the effectiveness of the simplified method. The adsorption process using ion-exchange resin in fixed bed column proved to be a promising method of IA recovering. An investigation using fermented broth must be made in further studies to determine an industrial scale model.

6. GENERAL CONCLUSION AND FUTURE OUTLOOK

The development of an efficient process for separating and purifying itaconic acid (IA) from fermentation broths face difficulties due to the high affinity of this hydrophilic solute for aqueous solutions and the complex composition of the fermentation broth.

The state of art of the IA recovering methods was described in Chapter 2. From that, it was concluded that crystallization not only requires a high input of energy, but also efficient removal of impurities. The separation by electrolysis, diafiltration and pertraction gives low yields due to loss of product in the effluent. Furthermore, the lifetime of the membranes may be relatively short due to hydromechanical wear. A major challenge for the successful separation of IA from fermentation broths is how to apply separation technology for industrial processes and lowering the cost on a large scale effectively while increasing productivity and revenue.

In search of a more practical method of IA determination, Chapter 3 described the selection to make the complexation experiments. The complexes formation with itaconate in the presence of transition metals could be confirmed with cobalt (II), nickel (II) and copper (II). However, the development of a method based on the formation of complexes with an absorbance distinct from that of the isolated components, essential to quantify the concentration of itaconate, was elusive, mostly because of errors due to small-angle curves developed from the absorbance-concentration curves. Good results were achieved in the complexation of itaconate with copper. However, problems such as metal precipitation and deprotonation of the acid occurred. Sodium nitrate was found to be the best solution for pH stabilization. Even though the determination of IA was not achieved on Chapter 3, in Chapter 4, the spectrophotometric reading at 240nm, which is quick and of easy handling, proved to be efficient when working on nearly pure concentrations. This was the method used to quantify soluble IA in this work.

Chapter 4 brought us that the relatively low solubility of calcium itaconate ensures that precipitation is feasible as a recovery method for IA from fermented broths. The low solubility of the salt, especially at elevated temperatures, allows the concentration of the free acid at high temperatures and precipitation as calcium salts

without the need of cooling. During the itaconate recovery, it was possible to achieve 99% yield using 100mM concentrations of sulfuric acid.

Chapter 5 defined the adsorption parameters of IA in commercial ion-exchange resins. The results showed that the *PFA-300* resin is a more effective adsorbent for IA removal from aqueous solutions. However, the *A-500P* resin presents a faster saturation rate compared with *PFA-300*.

From all that, it is possible to conclude that adsorption is a promising method for organic acids recovering. The well executed adsorption process tends to diminish the number of unit operations from the standard industrial method (FIGURE 2.2). A conceptual process flow using adsorption is presented in FIGURE 6.1.

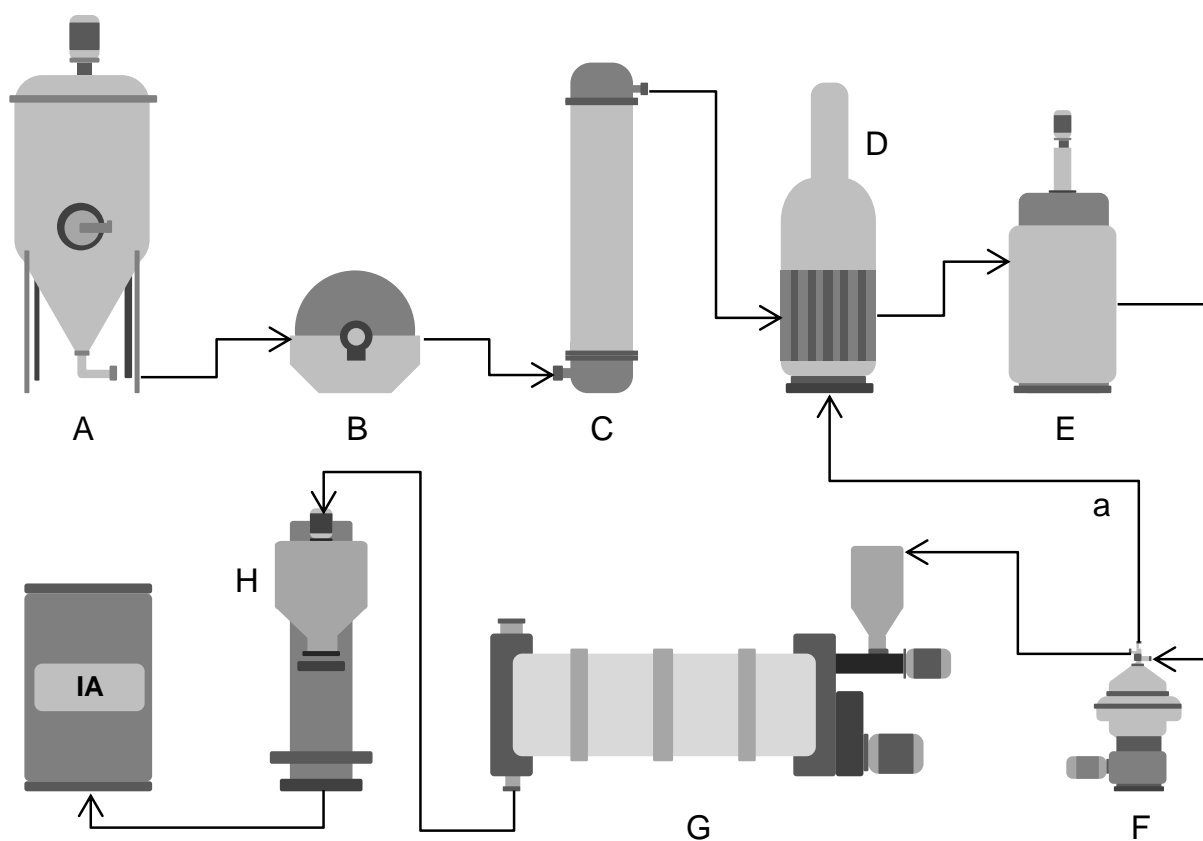


FIGURE 6.1. Process flow design of IA recovery process from fermentative broth with adsorption fixed bed column
 (A) bioreactor; (B) filter; (C) adsorption column; (D) evaporator; (E) crystallization; (F) separator; (G) drying shelves; (H) packaging; (a) second crystallization

7. REFERENCES

APELBLAT, A.; MANZUROLA, E. Solubilities of L-aspartic, DL-aspartic, DL-glutamic, p-hydroxybenzoic, o-anistic, p-anistic, and itaconic acids in water from T=278K to T=345K. *The Journal of Chemical Thermodynamics*. 29, 1527-1533, 1997.

ASÇI, Y. S.; INCI, I. A novel approach for itaconic acid extraction: Mixture of trioctylamine and tridodecylamine in diferente diluentes. *Journal of Industrial and Enginnering Chemistry*. 18, 1705-1709, 2012.

BIRD, R. B.; STEWART, W. E.; LIGHTFOOT, E. N. *Transport phenomena*, Revised 2nd edition, Hardcover, 2006.

BOUIS, P. A. *Reagent chemicals: Specifications and Procedures*. 3th edition, American Chemical Society Specifications, 2006.

BRESSLER, E.; BRAUN, S. Separation mechanisms of citric and itaconic acids by water-immiscible amines. *Journal of Chemical Technology and Biotechnology*. 74, 891-896, 1999.

CARSTENSEN, F.; KLEMENT, T.; BÜCHS, J. MELIN, T.; WESSLING, M. Continuous production and recovery of itaconic acid in a membrane bioreactor. *Bioresource Technology*. 137, 179-187, 2013.

CARSTENSEN, F.; MARX, C.; ANDRÉ, J.; MELIN, T. WESSLING, M. Reverse-flow diafiltration for continuous in situ product recovery. *Journal of Membrane Science*. 421-422, 39-50, 2012.

CUI, L.; XIE, P.; SUN, J. W.; YU, T.; YUAN, J. Q. Data-driven prediction of the product formation in industrial 2-keto-L-gulononic acid fermentation. *Computers & Chemical Engineering*. 36, 386-91, 2012.

DWIARTI, L.; OTSUKA, M.; MIURA, S. YAGUCHI, M. OKABE, M. Itaconic acid production using sago starch hydrolysate by *Aspergillus terreus* TN484-M1. *Bioresource Technology*. 98, 3329-3337, 2007.

FIDALEO, M.; MORESI, M. Application of the Nernst-Planck approach to model the electro-dialytic recovery of disodium itaconate. *Journal of Membrane Science*. 349, 293-404, 2010.

FREUNDLICH, H. Z. Die Bedeutung der adsorption bei der fällung der suspensionskolloide. *Zeitschrift für Physikalische Chemie - Stochiometrie und Verwandtschaftslehre*, 73, 385-423. 1910.

FRIEDKIN, M. Determination of Itaconic Acid in Fermentation Liquors. *Industrial and Engineering Chemistry*. 17, 637-638, 1945.

GLUSZSZ, P.; JAMROZ, T.; SENCIO, B.; LEDAKOWICZ, S. Equilibrium and dynamic investigations of organic acids adsorption onto ion-exchange resins. *Bioprocess Biosystems Engineering*. 26, 185-190, 2004.

GULICOVSKI, J. J.; CEROVIC, L. S.; MILONJIC, S. K.; POPOVIC, I. G. Adsorption of itaconic acid from aqueous solutions onto alumina. *Journal of the Serbian Chemical Society*. 73, 825-834, 2008.

HANO, T.; MATSUMOTO, M.; OHTAKE, T.; SASAKI, K.; HORI, F.; KAWANO, Y. Extraction equilibria of organic acids with tri-n-octylphosphineoxide. *Journal of Chemical Engineering of Japan*. 6, 734-738, 1990.

HARTFORD, C. G. Rapid spectrophotometric method for the determination of itaconic, citric, aconitic, and fumaric acids. *Analytical Chemistry*. 34, 426-428, 1962.

HO, Y. S.; MCKAY, G. A kinetic study of dye sorption by biosorbent waste product pith. *Resources, Conservation and Recycling*. 25, 171-193, 1999a.

HO, Y. S.; MCKAY, G. Kinetic models for the sorption of dye from aqueous solution by wood. *Institution of Chemical Engineers*. 76, 183-191, 1998.

HO, Y. S.; MCKAY, G. Pseudo-second order model for sorption processes. *Process Biochemistry*. 34, 451-465, 1999b.

HUANG, X.; LU, X.; LI, Y.; LI, X.; LI, J. J. Improving itaconic acid production through genetic engineering of an industrial *Aspergillus terreus* strains. *Microbial Cell Factories*. 13:119, 2014.

İNCI, İ.; BAYAZIT, Ş. S.; AŞÇI, Y. S., Separation of succinic acid from aqueous solution by alumina adsorption. *Journal of Chemical & Engineering Data*. 56, 4449-4453, 2011.

JUN, Y. S.; HUH, Y. S.; PARK, H. S.; THOMAS, A.; JEON, S. J.; LEE, E. Z.; WON, J. W.; HONG, W. H.; LEE, S. Y.; HONG, Y. K. Adsorption of pyruvic and succinic acid by amine-functionalized SBA-15 for the purification of succinic acid from fermentation broth. *Journal of Physical Chemistry C*. 111, 13076-13086, 2007.

KAUR, G.; ELST, K. Development of reactive extraction systems for itaconic acid: a step towards in situ product recovery for itaconic acid fermentation. *RSC Advances*. 4, 45029-45039, 2014.

KESHAV, A.; WASEWAR, K. L. Back extraction of propionic acid from loaded organic phase. *Chemical Engineering Science*. 65, 2751-2757, 2010.

KLEMENT, T.; BÜCHS, J. Itaconic acid - A biotechnological process in change. *Bioresource Technology*. 135, 422-431, 2013.

KOBAYASHI, T., NAKAMURA, I. Process for recovering itaconic acid and salts thereof from fermented broth. US Patent 693706, 1971.

KRIVANKOVA, I.; MARCISINOVÁ, M.; SÖHNEL, O. Solubility of Itaconic and Kojic Acids. *Journal of Chemical & Engineering Data*. 37, 23-24, 1992.

KUEZ, A.; GALLENMÜLLER, Y.; WILLKE, T.; VORLOP, K. D. Microbial production of itaconic acid: developing a stable platform for high product concentrations. *Applied Microbiology and Biotechnology*. 96, 1209-1216, 2012.

LANGMUIR, I. Chemical reactions at low pressures. *Journal of the American Chemical Society*, 37, 1139-1167, 1915.

LAWRANCE, G. A. *Introduction to Coordination Chemistry*. Wiley, 2010.

LI, A.; SACHDEVA, S.; URBANUS, J. H.; PUNT, P. In-stream Itaconic acid recovery from *Aspergillus terreus* fedbatch fermentation. *Industrial Biotechnology*. 3, 139-145, 2013.

LI, Q.; LI, W.; WANG, D.; LIU, B.; TANG, H.; YAMG, M.; LIU, Q.; XING, J.; SU, Z. pH neutralization while succinic acid adsorption onto anion-exchange resins. *Applied Biochemistry Biotechnology* 160, 438-445, 2010.

LOCKWOOD, L. B. Production of organic acids by fermentation. Part 3: Itaconic acid. *Microbial Technology*. 1, 367-373, 1975.

LÓPEZ-GARZÓN, C. S.; STRAATHOF, A. J. J. Recovery of carboxylic acids produced by fermentation. *Biotechnology Advances*. 32, 873-904, 2014.

MATSUMOTO, M.; OTONO, T.; KONDO, K. Synergistic extraction of organic acids with tri-n-octylamine and tri-n-butylphosphate. *Separation and Purification Technology*. 24, 337-342, 2001.

MCKINLAY, J. B.; VIEILLE, C.; ZEIKUS, J. G. Prospects for a bio-based succinate industry. *Applied Microbiology and Biotechnology*. 76, 727-740, 2007.

MILLER, C.; FOSMER, A.; RUSH, B.; MCMULLIN, T.; BEACOM, D.; SUOMINEN, P. Industrial production of lactic acid. In: Moo-Young, M. editor. *Comprehensive biotechnology*. 2nd ed. Elsevier, 179-188, 2011.

NAM, H. G.; PARK, K. M.; LIM, S. S.; MUN, S. Adsorption equilibria of succinic acid and lactic acid on Amberchrom CG300C resin. *Journal of Chemical & Engineering Data*. 56, 464-471, 2011.

OKABE, M.; LIES, D.; KANAMASA, S. Biotechnological production of itaconic acid and its biosynthesis in *Aspergillus terreus*. *Applied Microbiology and Biotechnology*. 84, 797-806, 2009.

PERELYGIN, V. M.; PODGORNOVA, N. M.; SITNIKOV, A. I. Temperature dependence of the dissociation constant and the product of activities for calcium hydroxide in aqueous solutions. *Russian Journal of Physical Chemistry*. 74, 1719-1721, 2000.

POOLE, L. J.; KING, C. J. Regeneration of carboxylic acid-amine extracts by back-extraction with an aqueous solution of a volatile amine. *Industrial & Engineering Chemistry Research*. 30, 923-929, 1991.

RAJORIYA, R. K.; PRASAD, B.; MISHRA, I. M.; WASEWAR, K. L. Adsorption of Benzaldehyde on Granular Activated Carbon: Kinetics, Equilibrium, and Thermodynamic. *Chemical and Biochemical Engineering Quarterly*. 21, 219-226, 2007

RAMAMOORTHY, S.; SANTAPPA, M. Spectrophotometric studies on complexes of Cu^{++} with malic and itaconic acids. *Journal of Inorganic and Nuclear Chemistry*. 30, 1855-1863, 1968.

RENNY, J. S.; TOMASEVICH, L. L.; TALLMADGE, E. H.; COLLUM, D. B. Method of continuous variations: Applications of Job plots to the study of molecular associations in organometallic chemistry. *Angewandte Chemie International Edition in English*. 52, 11998-12013, 2013.

ROBERTIS, A.; STEFANO, C.; RIGANO, C.; SAMMARTANO, S. Thermodynamic parameters for the protonation of carboxylic acids in aqueous tetraethylammonium iodide solutions. *Journal of Solution Chemistry*. 19, 569-587, 1990.

ROGERS, P.; CHEN, J. S.; ZIDWICK, M. J. Organic acid and solvent production part I: acetic, lactic, gluconic, succinic and polyhydroxyalkanoic acids. In: Dworkin, M. editor. *The prokaryotes*. Singapore: Springer, 511-755, 2006.

SAUER, M.; PORRO, D.; MATTANOVICH, D.; BRANDUARDI, P. Microbial production of organic acids: Expanding the markets. *Trends Biotechnology*. 26, 100-108, 2008.

SEADER, J. D.; HENLEY, E. J.; ROPER, D. K. *Separation Process Principles: Chemical and Biochemical Operations*. Wiley, 2010.

SOCCOL, C.R; VANDENBERGHE, L. P. S.; RODRIGUES, C.; PANDEY, A. New perspectives for citric acid production and application. *Food Technology Biotechnology*. 44, 141-449, 2006.

STODOLICK, J.; FEMMER, R.; GLOEDE, M.; MELIN, T.; WESSLING, M. Electrodialysis of itaconic acid: A short-cut model quantifying the electrical resistance in the overlimiting current density region. *Journal of Membrane Science*. 453, 275-281, 2014.

STRAATHOF, A. J. J. The proportion of downstream costs in fermentative production processes. In: Moo-Young, M. editor. *Comprehensive biotechnology*. 2nd ed. Elsevier. 811-814, 2011.

TIEN, C. Adsorption Calculations and Modeling. In: Brenner, H. editor. Elsevier. 1994.

WASEWAR, K. L.; SHENDE, D.; KESHAV, A. Reactive extraction of itaconic acid using quaternary amine Aliquat 336 in ethyl acetate, toluene, hexane, and kerosene. *Industrial & Engineering Chemistry Research*. 50, 1003-1011, 2011b.

WASEWAR, K. L.; SHENDE, D.; KESHAV, A. Reactive extraction of itaconic acid using tri-n-butyl phosphate and Aliquat 336 in sunflower oil as a non-toxic diluent. *Journal of Chemical Technology and Biotechnology*. 86, 319-323, 2011a.

WILLKE, T.; VORLOP, K. D. Biotechnological production of itaconic acid. *Applied Microbiology Biotechnology*. 56, 289-295, 2001.

WU, F. C.; TSENG, R. L.; HUANG, S. C.; JUANG, R. S. Characteristics of pseudo-second-order kinetic model for liquid-phase adsorption: A mini-review. *Chemical Engineering Journal*. 151, 1-9, 2009.

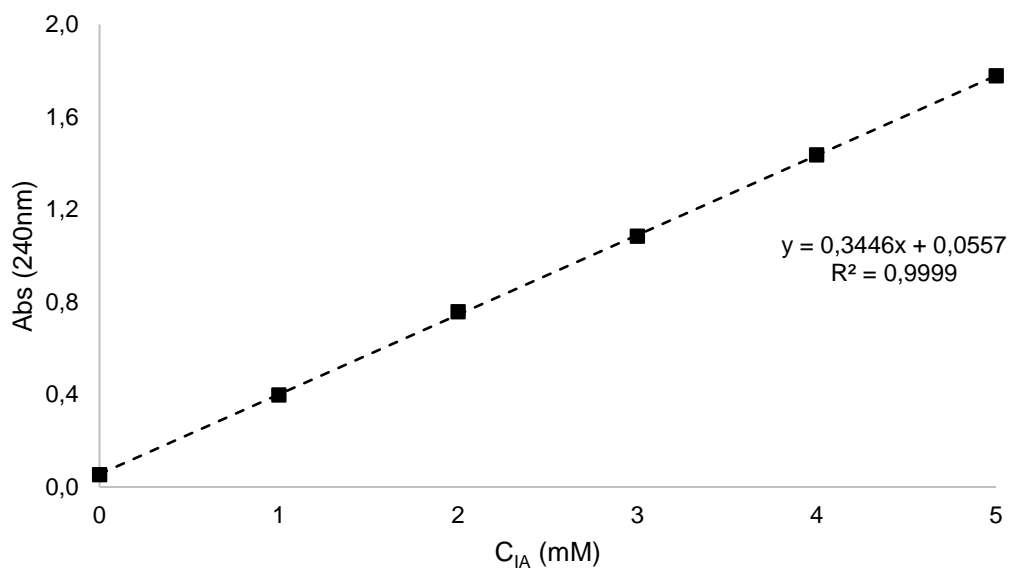
XU, Z.; CAI, J. G.; PAN, B. C. Mathematically modeling fixed-bed adsorption in aqueous systems. *Journal of Zhejiang University-Science A (Applied Physics & Engineering)* 14, 155-176, 2013.

ZAKI, M. T. M.; ALQASMI, R. Spectrophotometric determination of copper (II) as citrate or EDTA complex. *Fresenius' Zeitschrift für Analytische Chemie*. 306, 400, 1981.

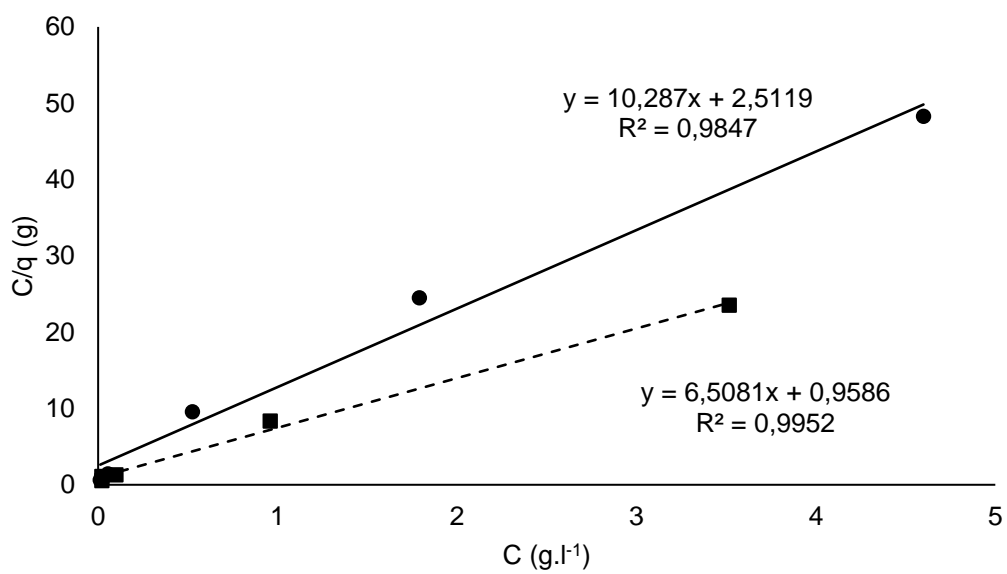
ZHANG, X. X.; MA, F.; LEE, D. J. Recovery of itaconic acid from supersaturated waste fermentation liquor. *Journal of the Taiwan Institute of Chemical Engineers*. 40, 583 - 585, 2009.

APPENDIX

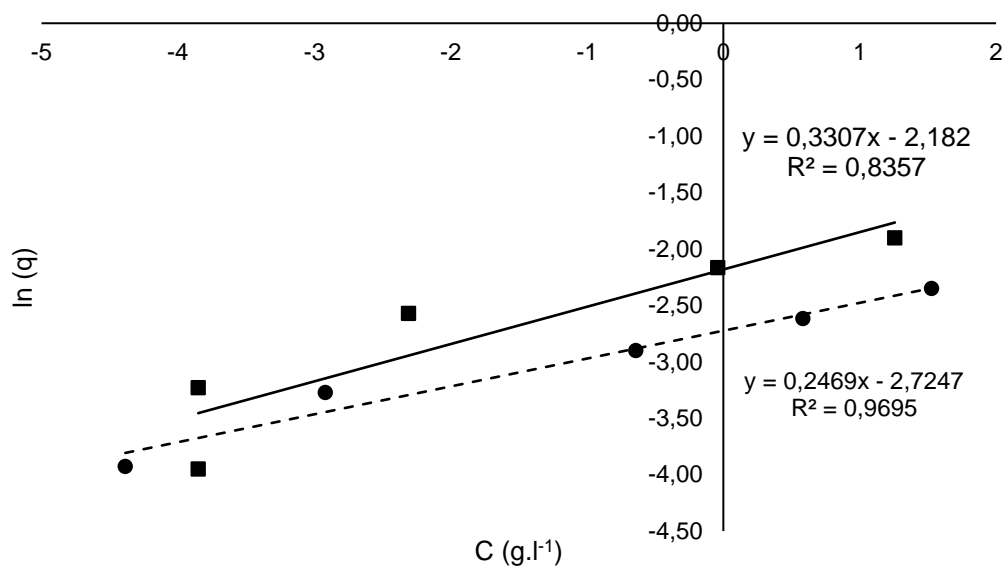
IA concentration curve:



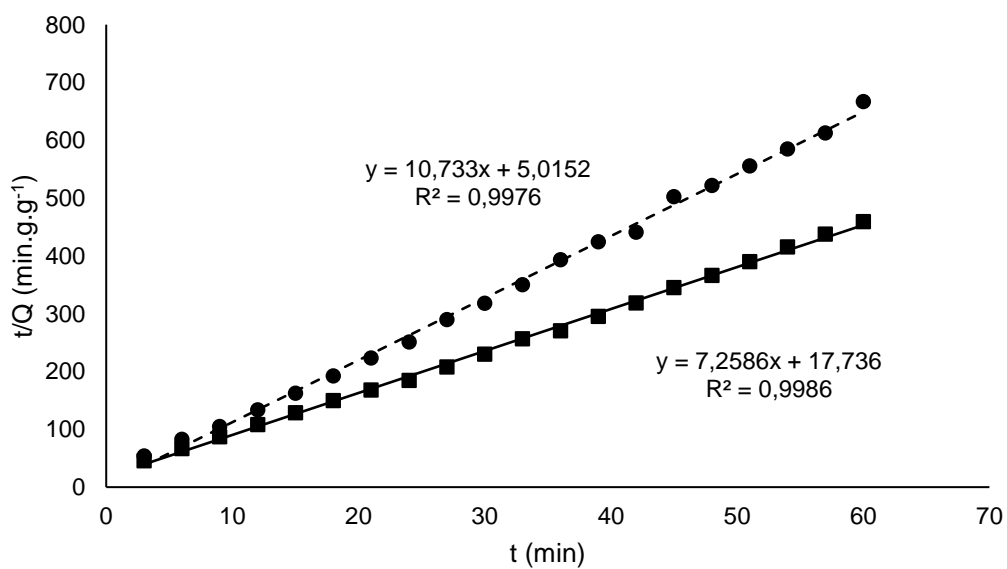
Linearization of the Langmuir isotherm:



Linearization of the Freundlich isotherm:



Linearization of the pseudo second order kinetics:



APPENDIX

Algorithm of mathematical shortcut model used in software MATLAB:

```

time = input(' Input the experimental data to time in [sg]: ');
IA   = input(' Input the experimental data to concentration of itaconic
acid in [g/L] ');

lin  = 10;
Alt  = input('Input the high of column in [dm]: ')

deltaZ = Alt/lin;          % Numerical value for difference finite

% Operation parameters

Fluxo  = 1.388e-5;        % volumetric flow of itaconic acid [dm^3.s^-1]
Eb     = 0.32;           % Porosity of column packed
Dz     = 1.5832e-5;      % Axial dispersion coefficient [dm^2.s^-1]
vz     = 3.5903e-4;      % lineal velocity of solute [dm.s^-1]
Rp     = 0.68e-3;        % Radio media of particles

% Initial conditions
Co = 52.04;              % inicial concentration of itaconic acid [g.dm^-3]
Cf = zeros(lin,1);
Cf(1)=Co;
to = 0;
tf = 120*60;
Vc = [Cf q];
K = [Dz Vz Eb]

Kop    = fminsearch(@(K)
objective_function(deltaZ,lin,C,Vc,Eb,time,IA,K),K);

Dl = Kop(1)
Vz = Kop(2)
Eb = Kop(3)
[t,C] = ode45(@(t,Vc) edospatial_1(deltaZ,lin,Co,Dl,Vz,Eb,Vc,t),[to
tf],Vc);

function [EDOS] = edospatial_1(deltaZ,lin,Co,Dl,Vz,Eb,Vc,t)
i=1;

Cf = Vc(1:lin);

while i<=lin
    if i == 1
        % difference finite forward of first order
        dCdZ(i,1) = Vz.*(Co-Cf(1))./-Dl;
        d2CdZ2(i,1) = (Cf(i+2) - 2*Cf(i+1) + Cf(i))/(deltaZ^2);
        i = i + 1;
    elseif i>1 && i < lin
        % difference finite of second order, central for internal nodes

```

```

        dCdZ(i,1) = (Cf(i+1)-Cf(i-1))/(2*deltaZ);
        d2CdZ2(i,1) = (Cf(i+1) - 2*Cf(i) + Cf(i-1))/(deltaZ^2);
        i = i + 1;
    else
        dCdZ(i,1) = (Cf(i)-Cf(i-1))/deltaZ;
        d2CdZ2(i,1) = (Cf(i) - 2*Cf(i-1) + Cf(i-2))/(deltaZ^2);
        i = i + 1;
    end
end
end

EDOS1= D1.*d2CdZ2 - Vz.*dCdZ;

function [Fob]=objective_function(deltaZ,lin,Co,Vc,Eb,time,IA,K)

D1 = K(1);
Vz = K(2);
Eb = K(3);
[t,C] = ode15s(@ (t,Vc) edospatial_1(deltaZ,lin,Co,D1,Vz,Eb,Vc,time);
Cc=C(:,lin)';

Fob = sum((Cc-IA).^2);

end

```